

March 4, 2004

Analysis of MM5 Simulations based on three PBL schemes over the eastern US for August 6 to 16, 2002

Winston Hao, Mike Ku, and Gopal Sistla
NYSDEC-DAR
Albany, NY 12233

Introduction: In a prior report¹ dated December 8, 2003, a comparison was performed between meteorological measurements and the simulated MM5 fields for August 6 to 16, 2002 based upon 3 approaches to the PBL. In this report, we provide the comparison with TDL and CASTNet measurements.

Purpose: The intent of this exercise was to investigate the response of three PBL schemes and develop a recommendation for the use of a PBL method for developing meteorological fields for the May through September of 2002, in support of air quality modeling work.

Approach: In this study, Prof. Dalin Zhang of University of Maryland, applied 3 PBL schemes for the August 6 to 16, 2002, a period in which the OTR experienced high ozone as well as particulate levels. The three schemes were (a) modified Blackadar [BL], (b) the Pleim-Xiu scheme with the soil module [PX], and (c) modified Blackadar with soil module [SSIB]. The simulated meteorological fields were compared to the measurements from TDL (NWS) and CASTNet.

Model setup: The MM5 model setup is similar to the earlier exercise of developing meteorological fields for July 1997, with the first level at 10 m. The projection for this exercise was that recommended by the RPOs, and has a spatial resolution of 12 km (see Figure 1)

Analysis: The basic approach used is to compare domain-wide averaged measurements and predictions for surface temperature, wind speed and direction, and where available with humidity. While the CASTNet sites are more representative of rural areas, the TDL are reflective of urban/suburban settings. There are 47 CASTNet and about 600 NWS sites in the TDL data set over the modeling domain.

TDL data and MM5 simulations:

Average wind speed and direction (see Figures 2a through 2c)

¹ Hao, W., Ku, M., and Sistla, G. (2002) 'Preliminary analysis of MM5 simulations for the August 6 to 17, 2002 – A status report', NYSDEC, Albany, NY 12233

Overall, the 3 PBL schemes provide good agreement with the observed average wind direction . In terms of wind speed:

BL: Under prediction of daytime maximum wind speed, but agreement with nighttime low windspeed

P-X: Systematic under prediction during daytime and over prediction in the nighttime

SSIB: Under prediction during daytime with phase lag, the predicted maximum occurring latter than the measured maximum

Temperature (see Figures 3a through 3c)

BL: Good agreement throughout the episode days

P-X: Initial over prediction of temperature minimum, and under prediction of daytime maximum

SSIB: Over prediction of daytime maximum

Humidity (see Figures 4a through 4c)

BL: While the general trend is captured during the episode, there is poor agreement between the observed and predicted diurnal patterns, with the observation showing a double peak versus one peak based on predictions.

P-X: The model yields the observed daily double peak, but with underprediction and a phase lag.

CASTNet data and MM5 simulations:

Average wind speed and direction (see Figures 5a through 5c)

All 3 PBL approaches provide good agreement with the observed average wind direction. In terms of wind speed:

BL: Wind speed over prediction during the daytime, a feature that differs from the TDL results, but good agreement with nighttime minimum

P-X: Wind speed over prediction, for both day- and nighttime hours.

SSIB: Wind speed over prediction at the start and end of the episode, and exhibiting a phase-lag of 1 to 2 hours

Average Temperature (see Figures 6a through 6c)

BL: Overall good agreement

P-X: Systematic under prediction during daytime and over prediction in the nighttime with phase lag

SSIB: Over prediction during the daytime, but good agreement during nighttime

Average Humidity

There were no data to perform this comparison, as mixing ratio cannot be estimated due to lack of station pressure.

Spatial distribution of correlation between TDL data and MM5 simulations

Wind Speed (see Figures 7a through 7c)

BL: The correlation levels are generally in the 0.7 or higher range over most portions of the domain, with lower values mainly confined to the southeastern and western parts of the domain.

P-X: The correlation levels are slightly lower compared to BL, with more stations exhibiting a correlation level of less than 0.6 in the Southeastern portion of the domain.

SSIB: The correlation levels are similar to P-X, but with increased number of stations exhibiting correlation levels less than 0.6 over the domain

Temperature (see Figures 8a through 8c)

BL: The correlation levels are generally higher (>0.97) over the northeastern portions of the domain, with the remainder of the domain exhibiting correlation levels in the range of 0.94 to 0.96

P-X: Overall the correlation levels are slightly lower than BL

SSIB: Similar to P-X, with correlation levels in the 0.95 throughout the domain

Humidity (see Figures 9a through 9c)

BL: The correlation levels over the northeast are generally higher than the rest of the domain, although most portions of the domain report correlation of 0.70 or higher

P-X: The correlation levels are comparable or slightly better than BLK

SSIB: The correlation levels are comparatively lower than the other two over the northeastern portions of the domain

Discussion and conclusions

On an overall basis, it appears that the BL scheme exhibits a better correspondence to the measured data than the other two schemes. The exception being the poor capture of the observed diurnal pattern of humidity in the case of the BL scheme. While the P-X scheme shows a better correspondence with the observed diurnal pattern for humidity, it fails to perform well for wind speed and temperature. Further work is needed to improve the performance of these methods. An examination of other studies in which the P-X scheme was applied suggests the predictive performance is similar to this study.

Other comparisons of model to observed or measured parameters such as cloud cover, precipitation, and upper air soundings/profiler network are under examination to provide a comprehensive evaluation of the meteorological model. Also, the use of the model simulated fields in air quality model and comparison to pollutant fields is also in progress.

Figure 2a MM5 Simulation - UMD BLK & TDL - Aug 6 01Z to Aug 17 00Z 2002

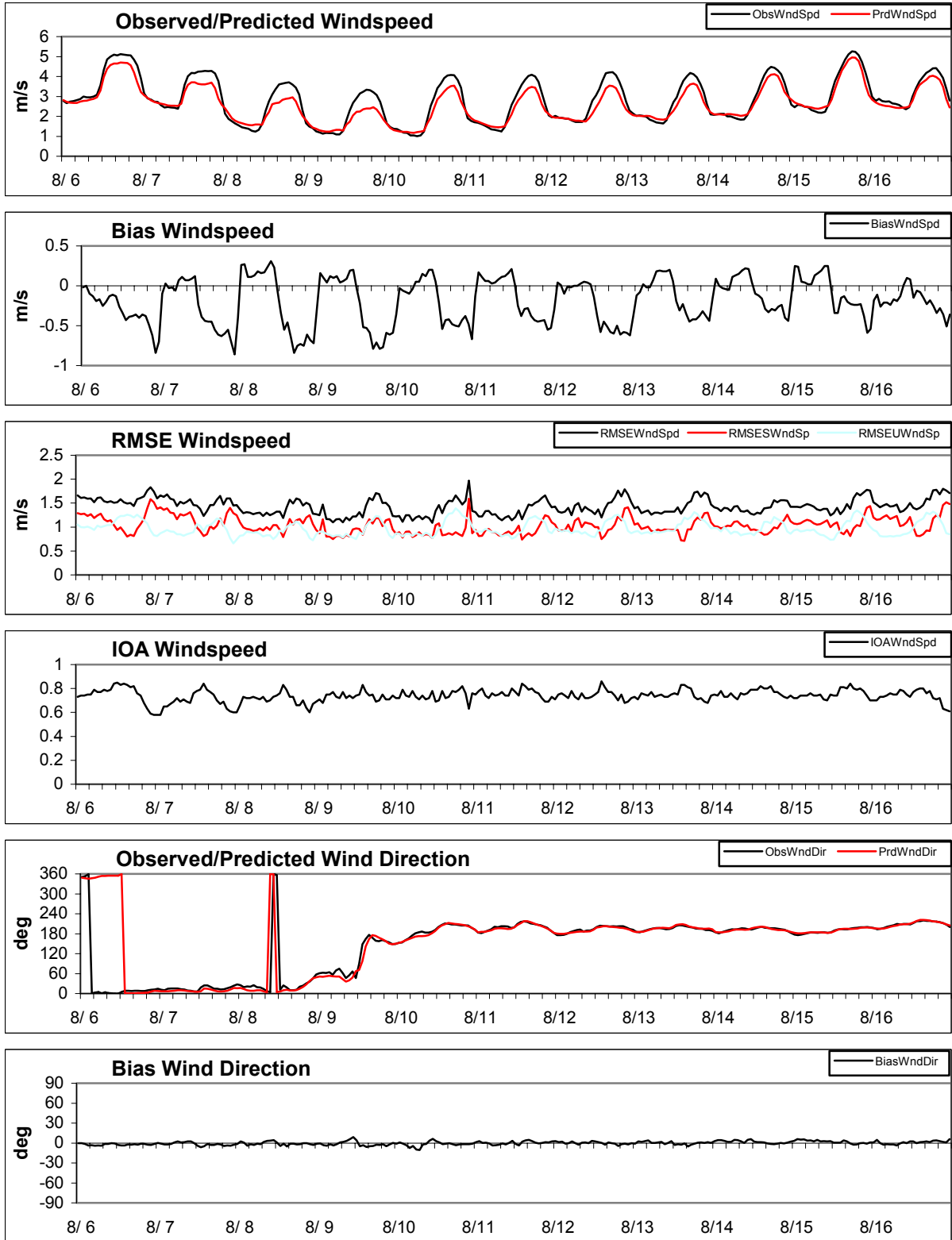


Figure 2b MM5 Simulation - UMD PX & TDL Aug 06 01Z to Aug 17 00Z 2002

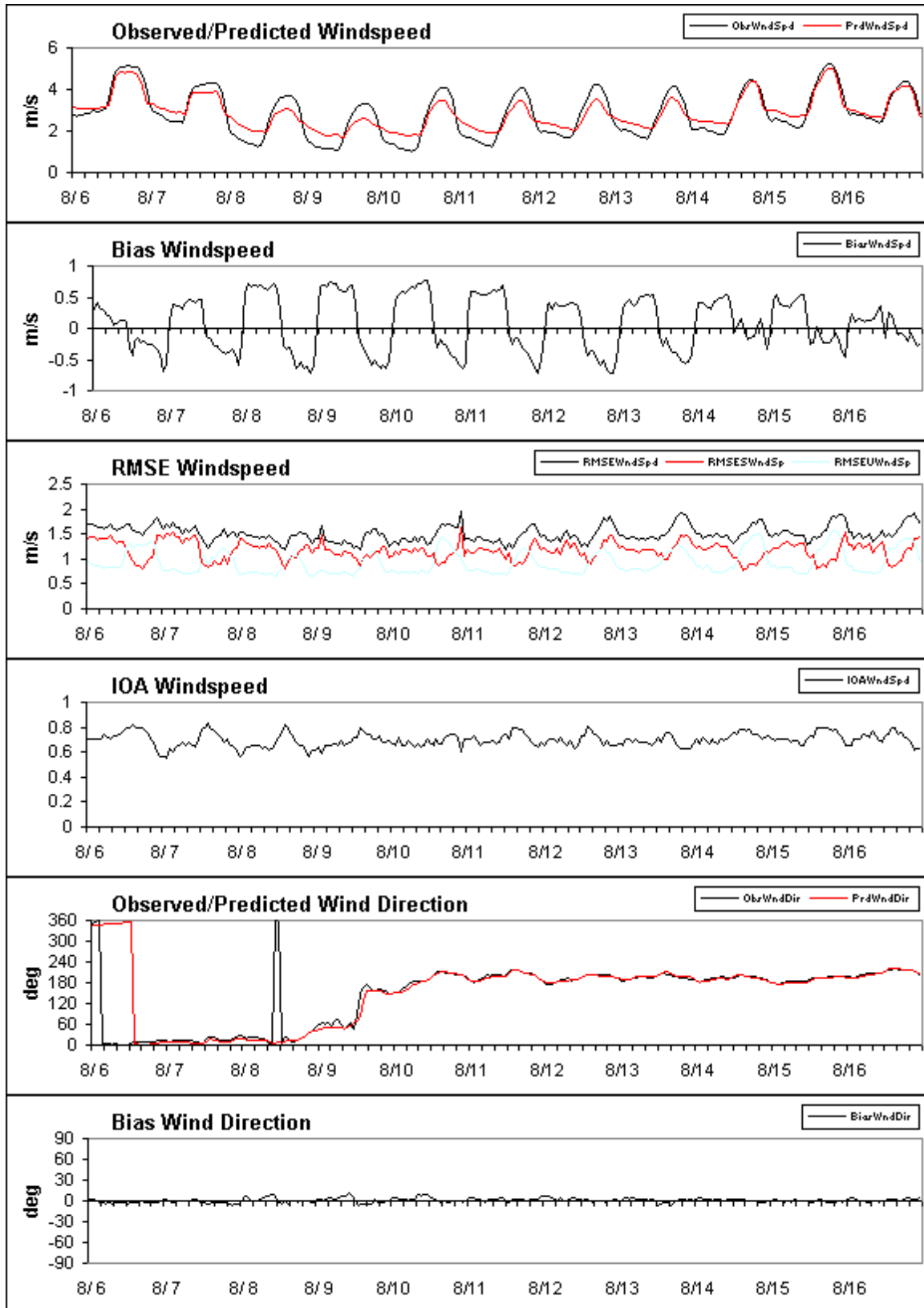


Figure 2c MM5 Simulation - UMD SSIB & TDL Aug 06 01Z to Aug 17 00Z 2002

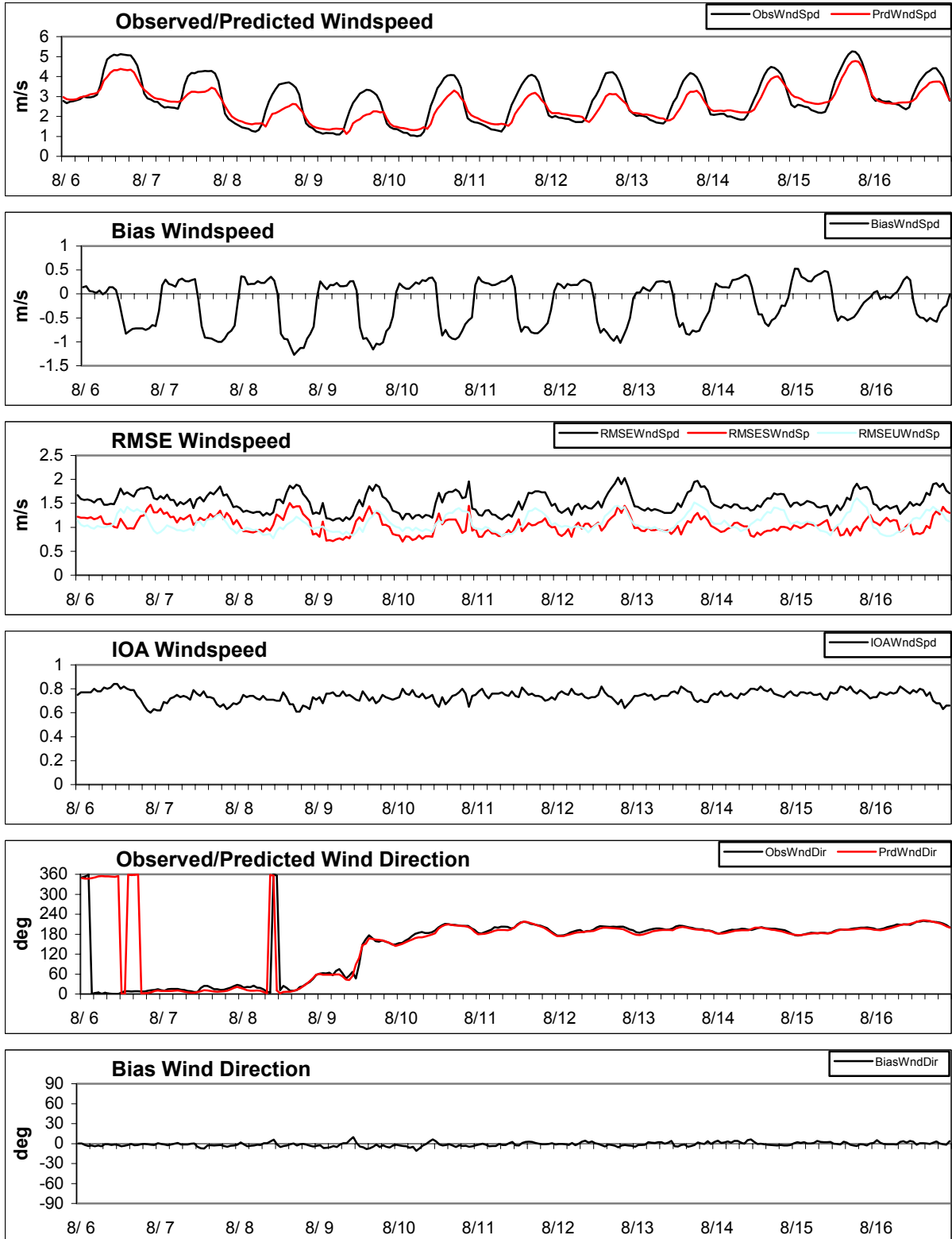


Figure 3a MM5 Simulation - UMD BL & TDL Aug 6 01Z to Aug 17 00Z 2002

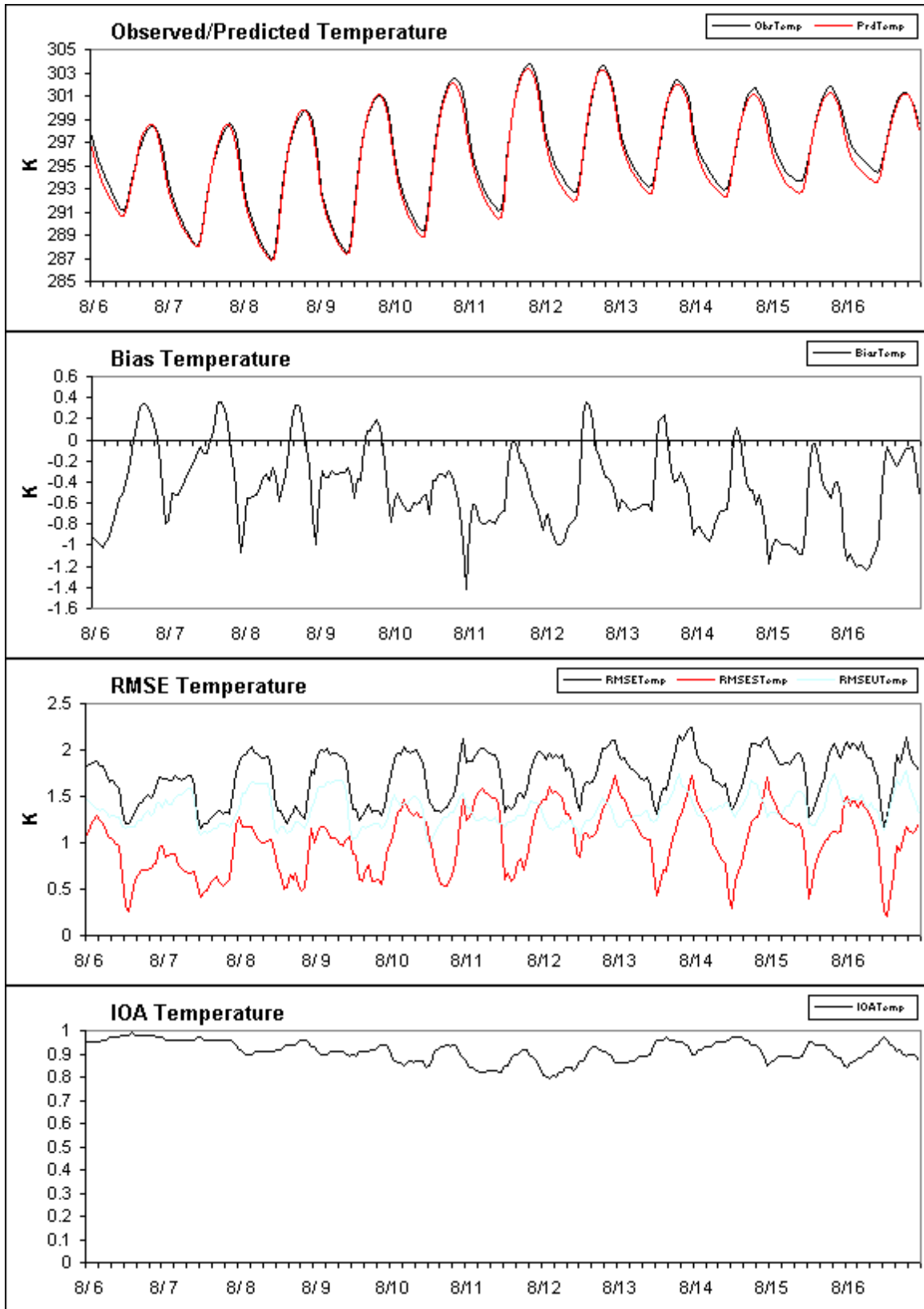


Figure 3b MM5 Simulation - UMD PX & TDL Aug 06 01Z to Aug 17 00Z 2002

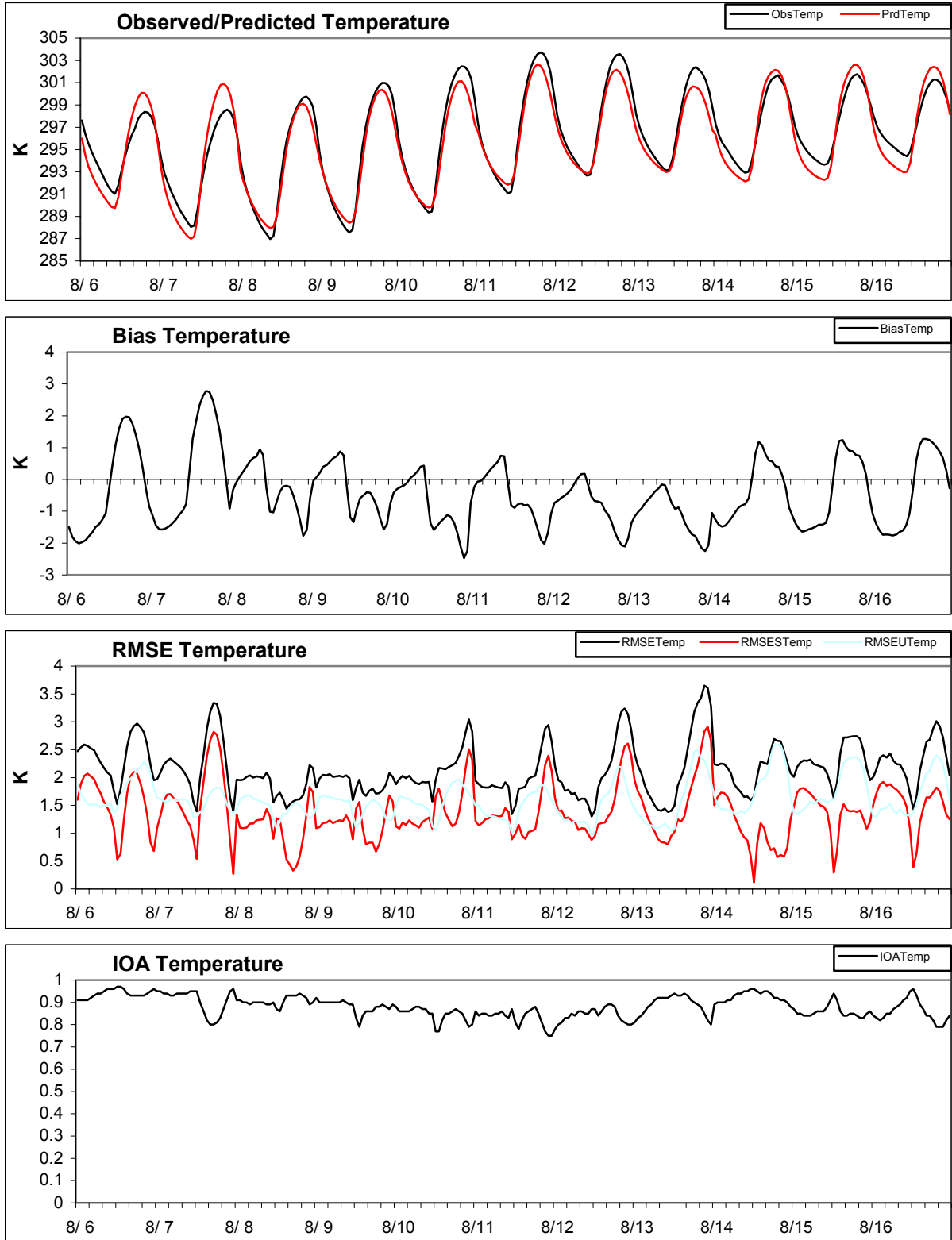


Figure 3c MM5 Simulation - UMD SSIB & TDL Aug 06 01Z to Aug 17 00Z 2002

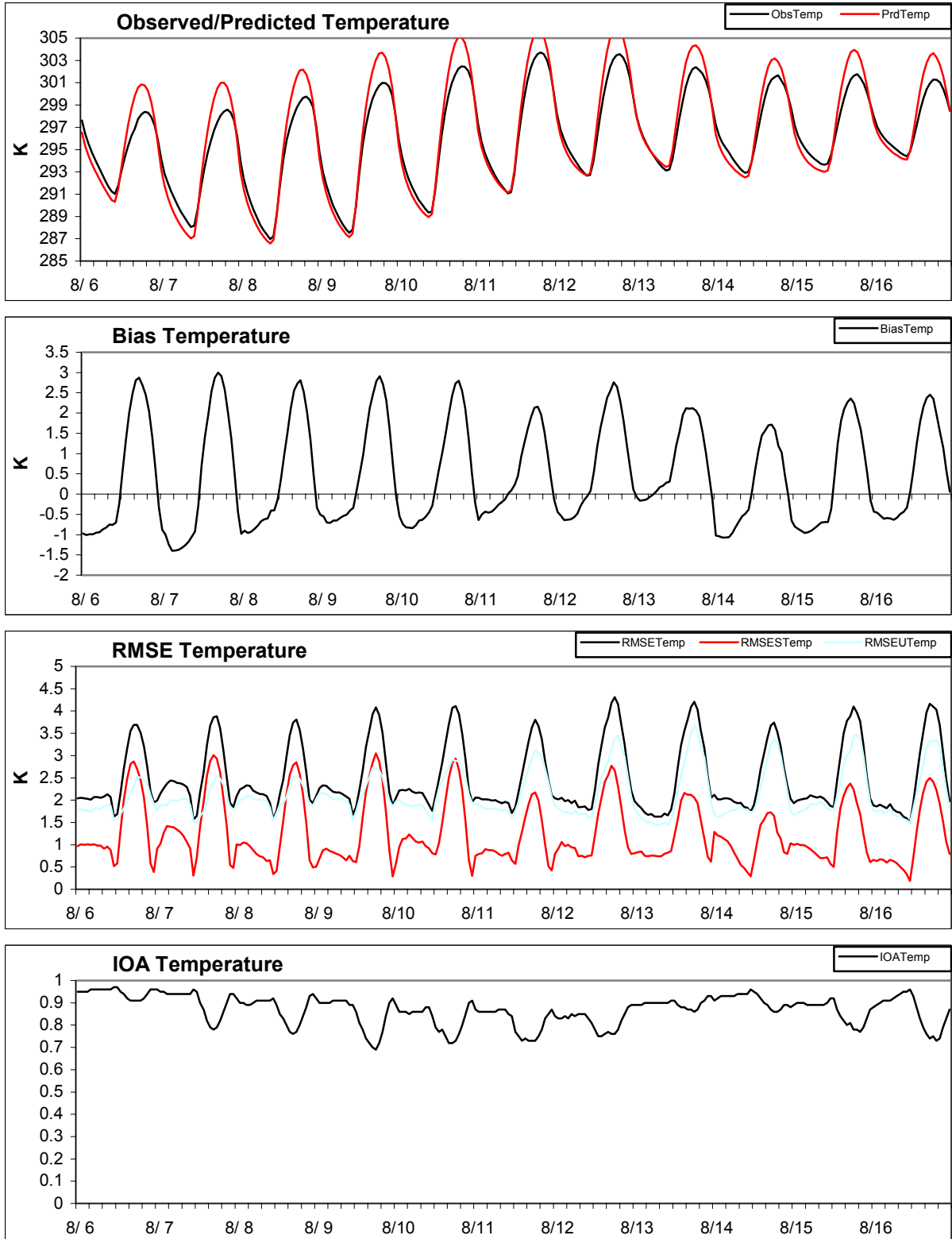


Figure 4a MM5 Simulation - UMD BL & TDL Aug 6 01Z to Aug 17 00Z 2002

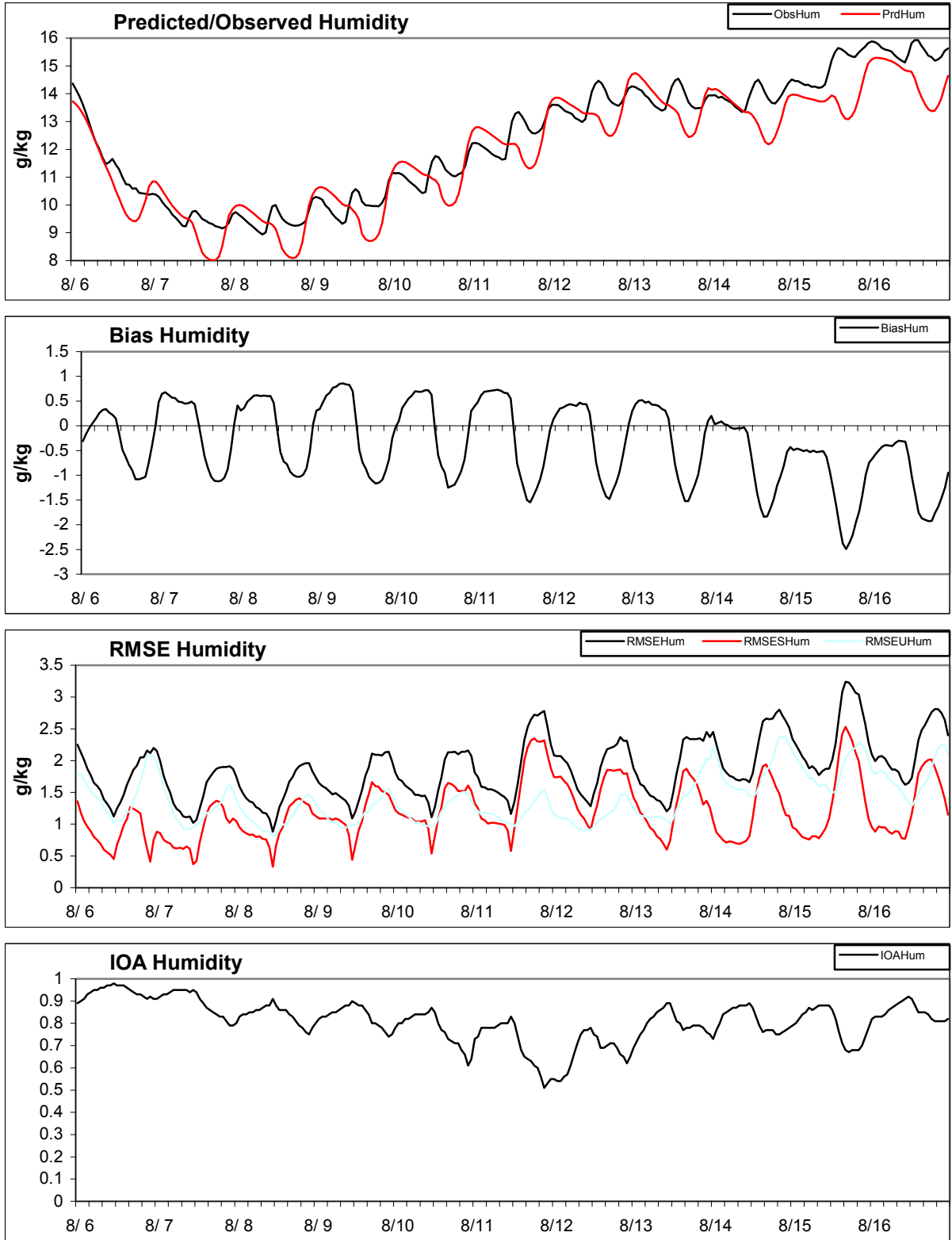


Figure 4b MM5 Simulation - UMD PX Aug 06 01Z to Aug 17 00Z

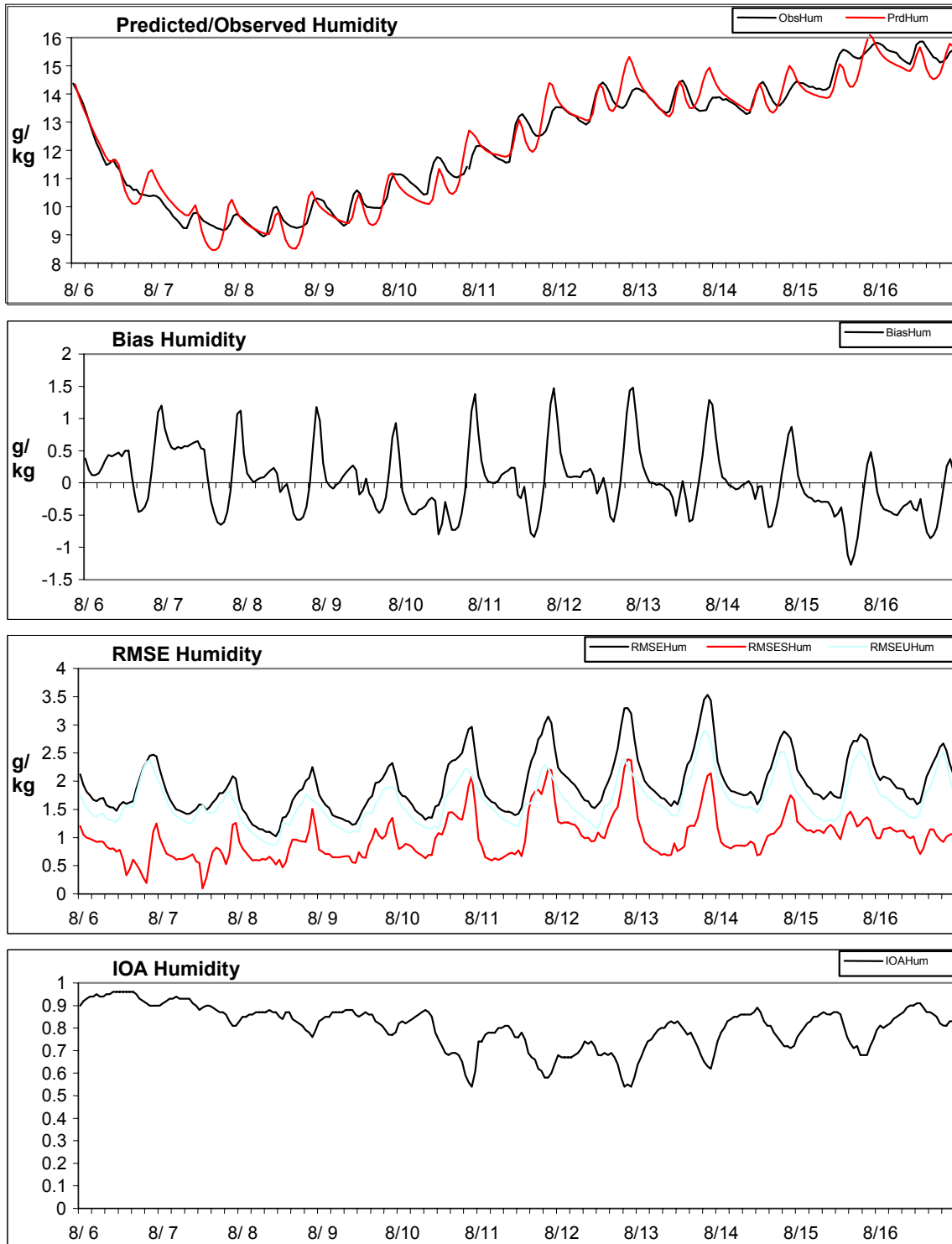


Figure 4c MM5 Simulation - UMD SSIB & TDL Aug 06 01Z to Aug 17 00Z 2002

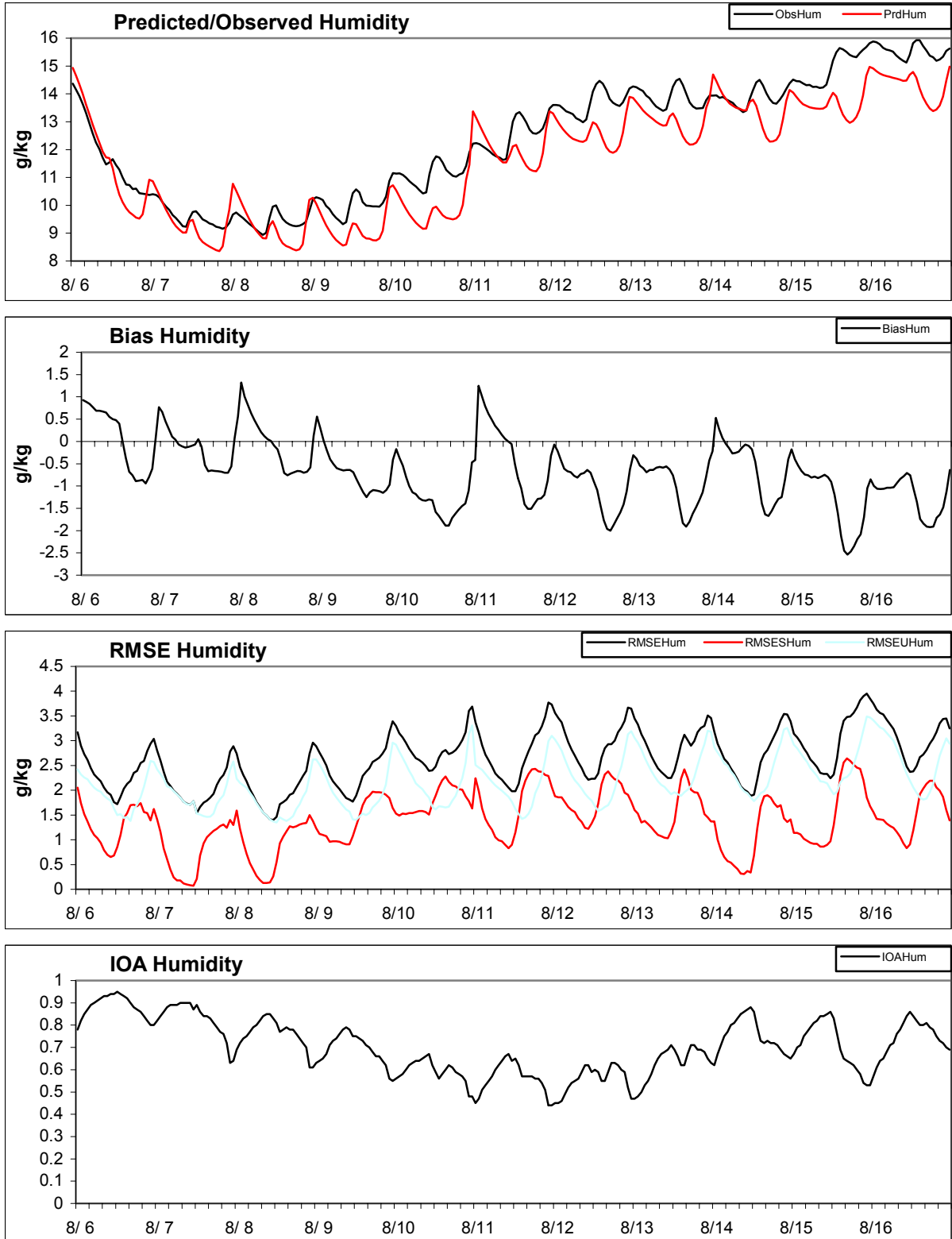


Figure 5a MM5 UMD - BL & CASTNet Aug 6 01Z to Aug 17 00Z 2002

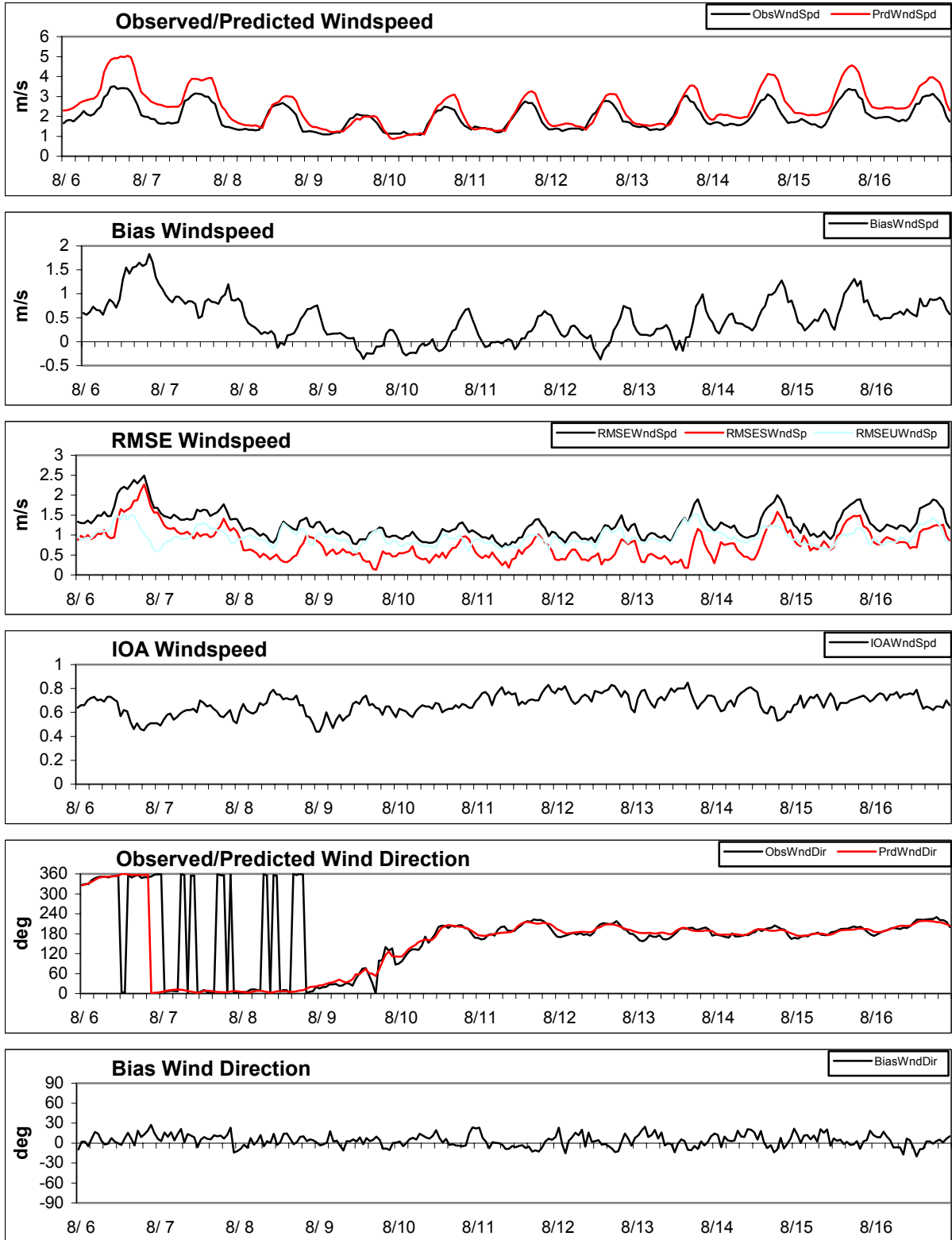


Figure 5b MM5 - UMD PX & CASTNet Aug 06 01Z to Aug 17 00Z 2002

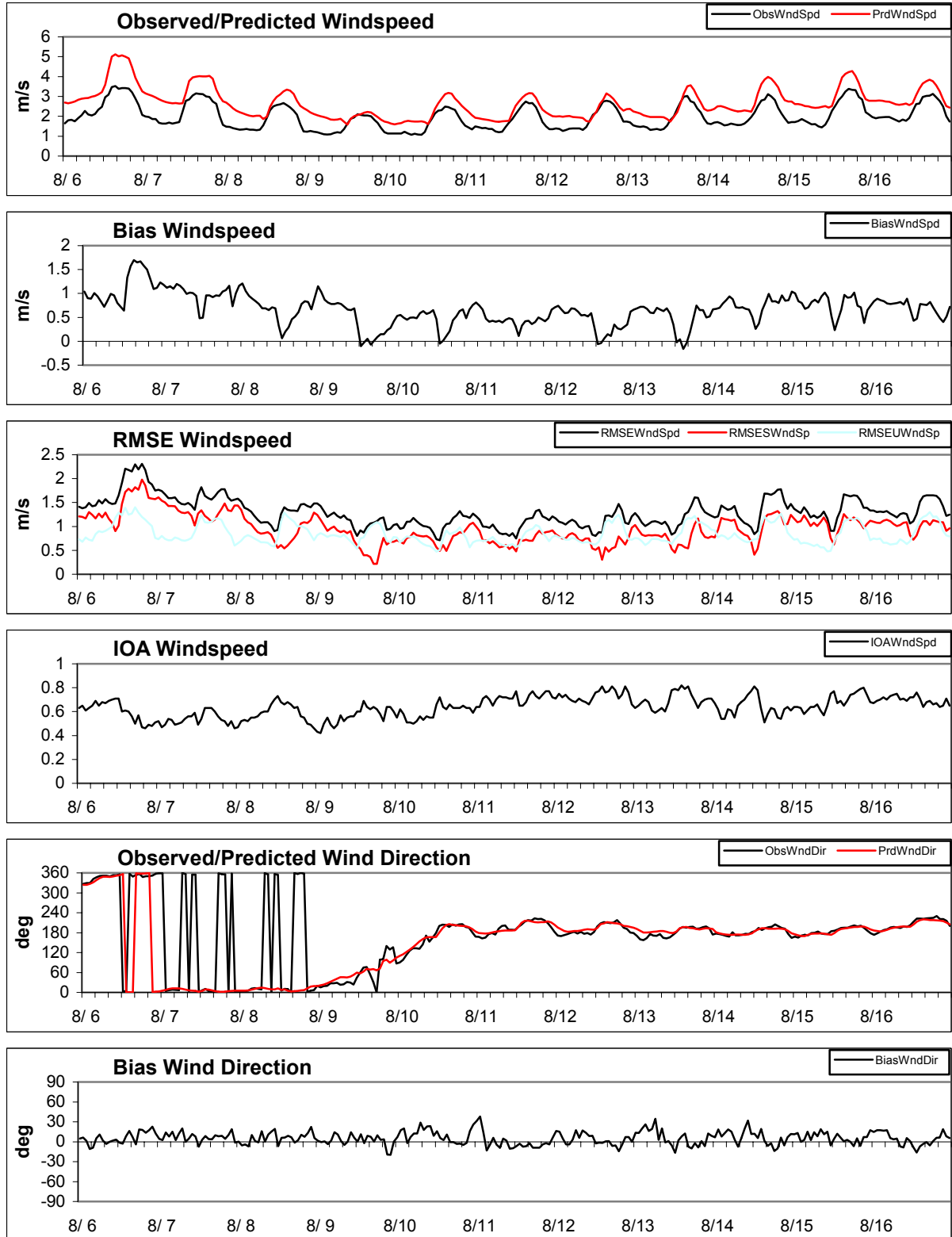


Figure 5c MM5 - UMD SSIB & CASTNet Aug 06 01Z to Aug 17 00Z 2002

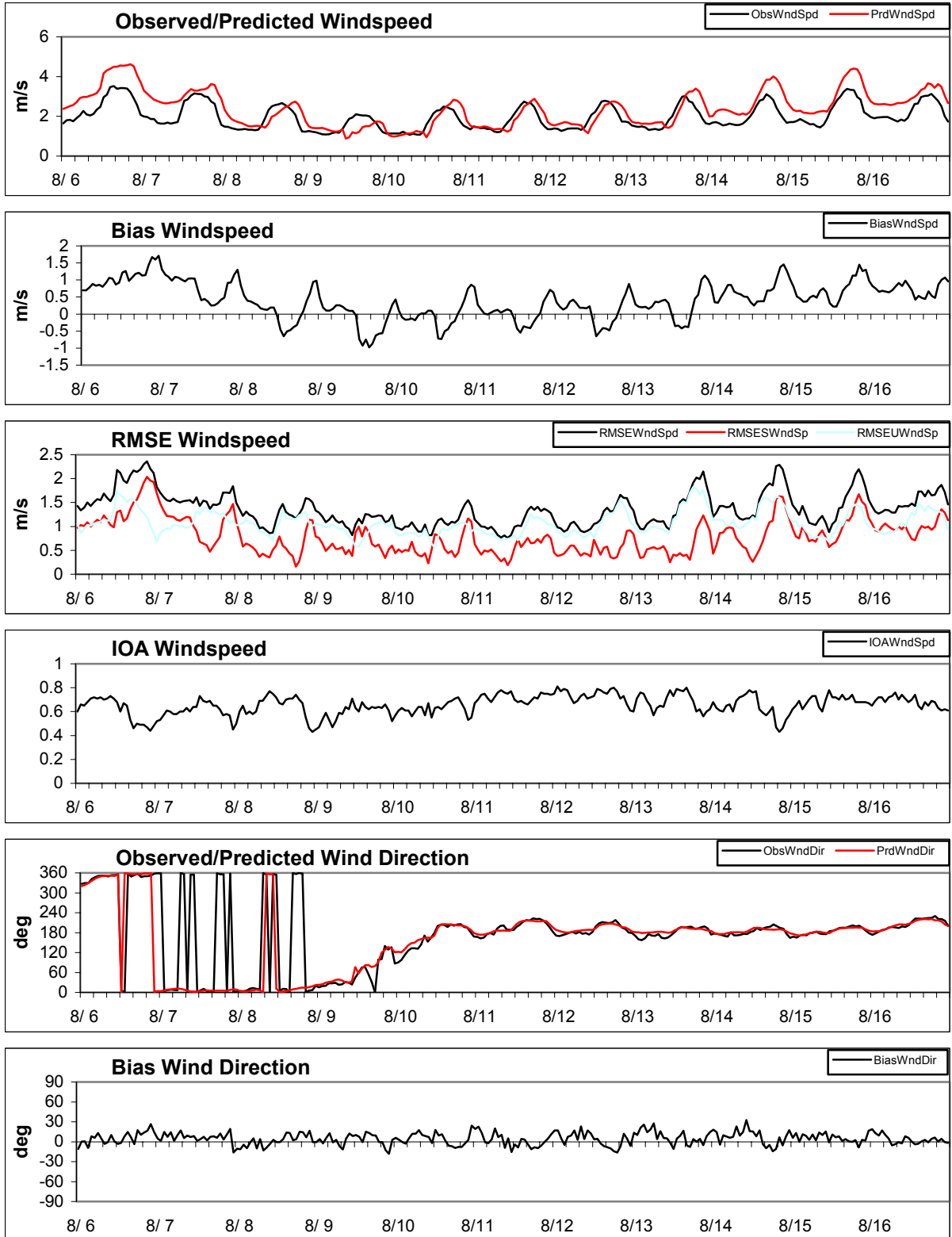


Figure 6a MM5 - UMD BL & CASTNet Aug 6 01Z to Aug 17 00Z 2002

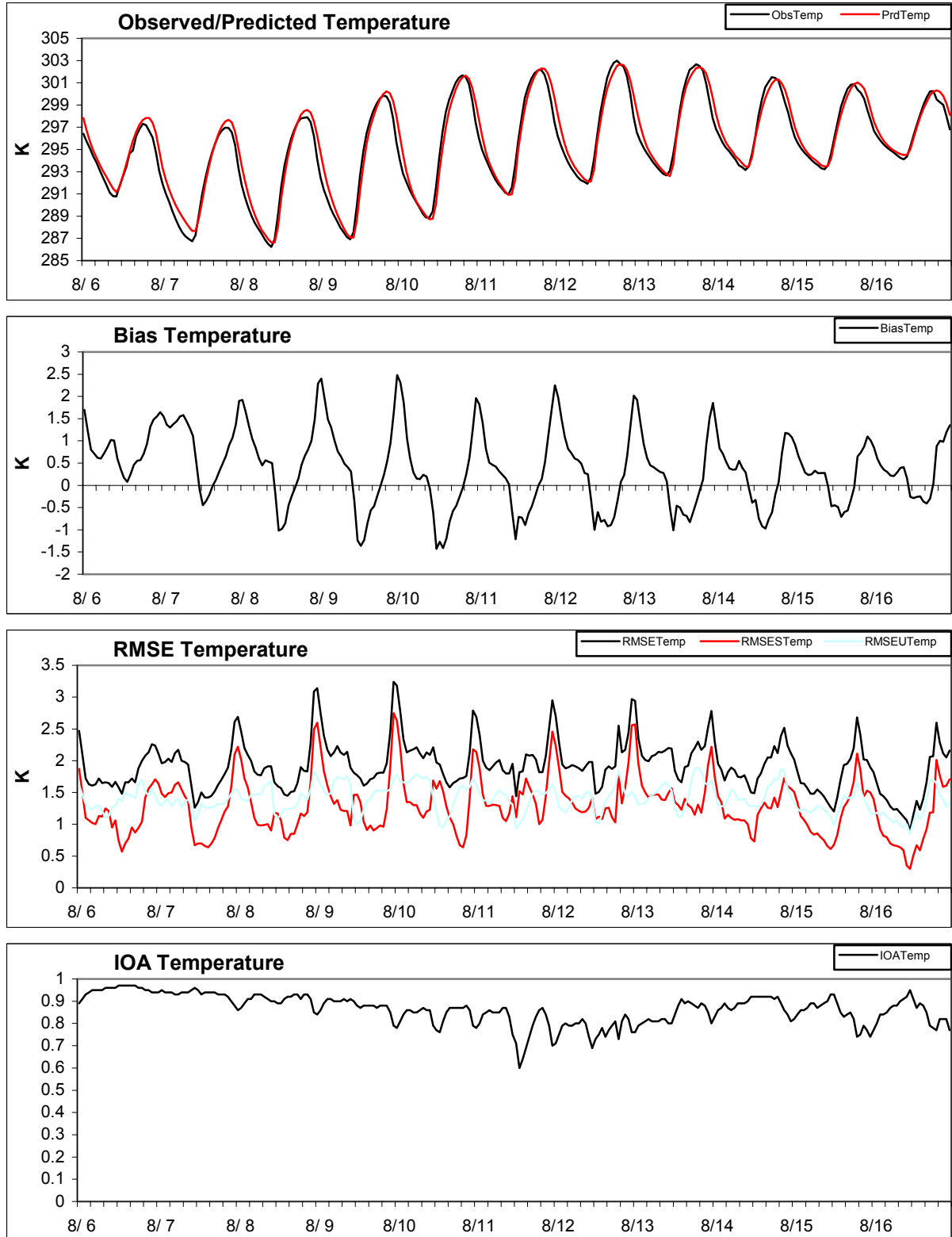


Figure 6b MM5 - UMD PX & CASTNet Aug 06 01Z to Aug 17 00Z 2002

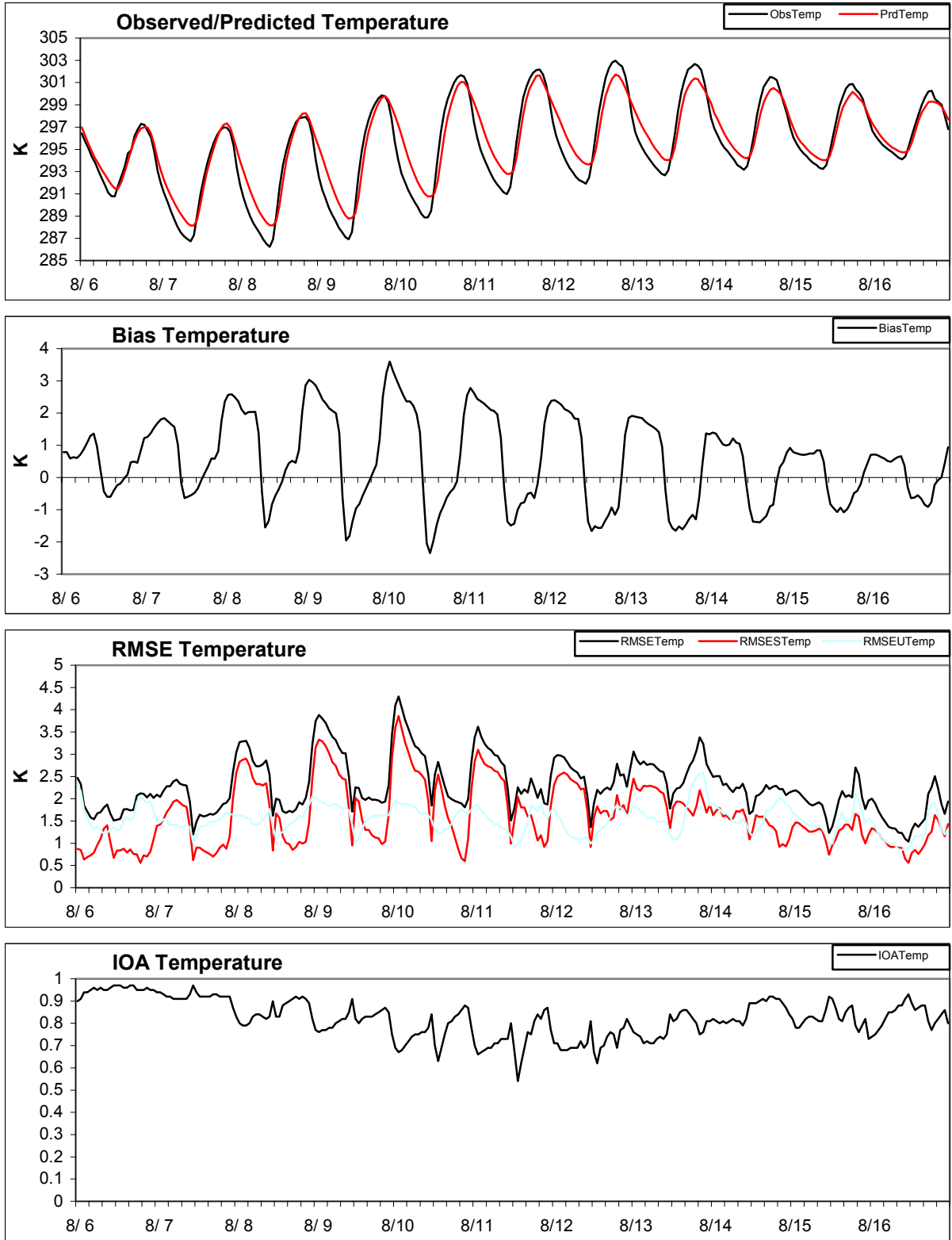


Figure 6c MM5 - UMD SSIB & CASTNet Aug 06 01Z to Aug 17 00Z 2002

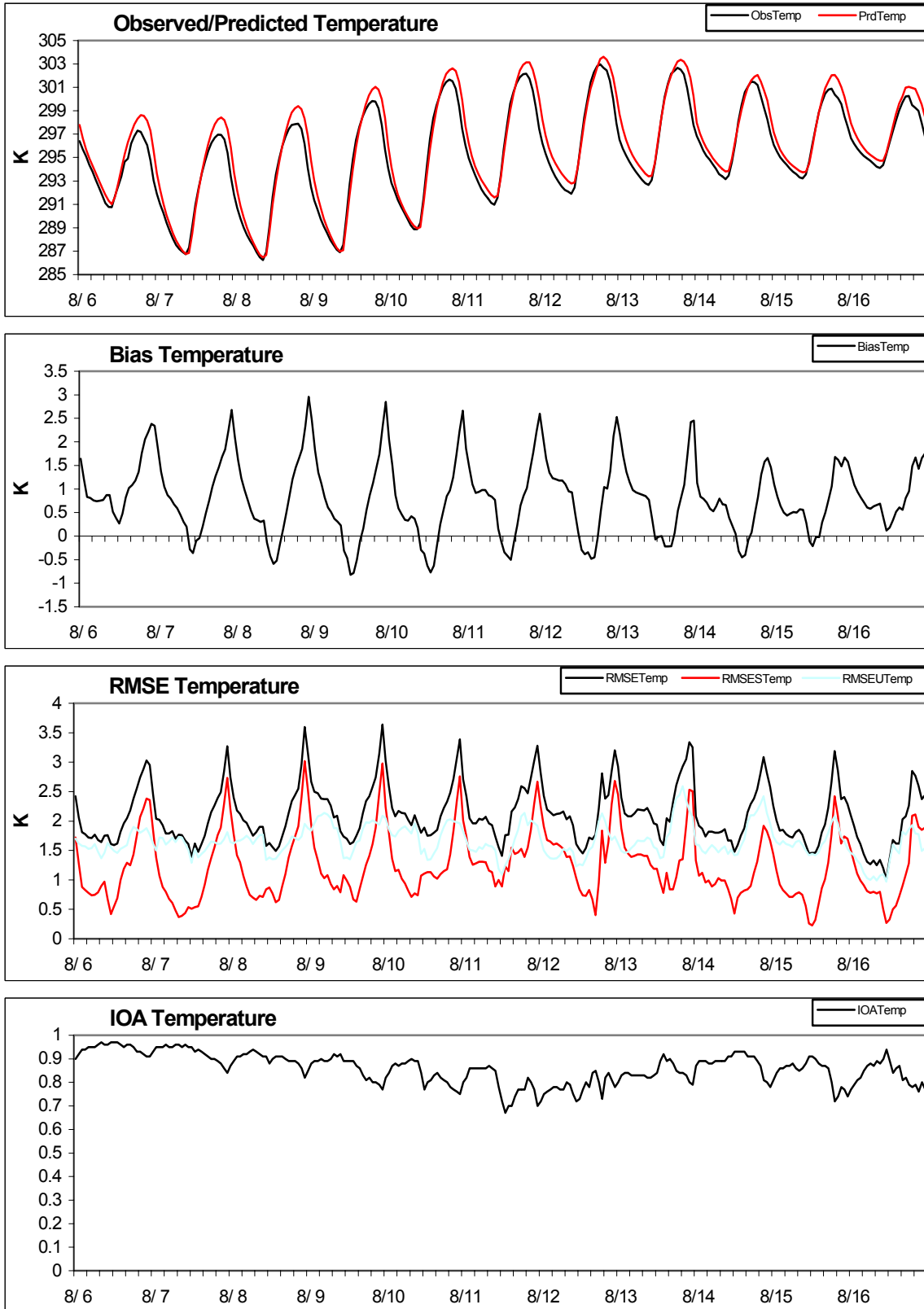


Figure 7a Spatial Correlation – Wind speed – BL & TDL

UMD 2002 MM5 BL Wind Speed Correlation with TDL

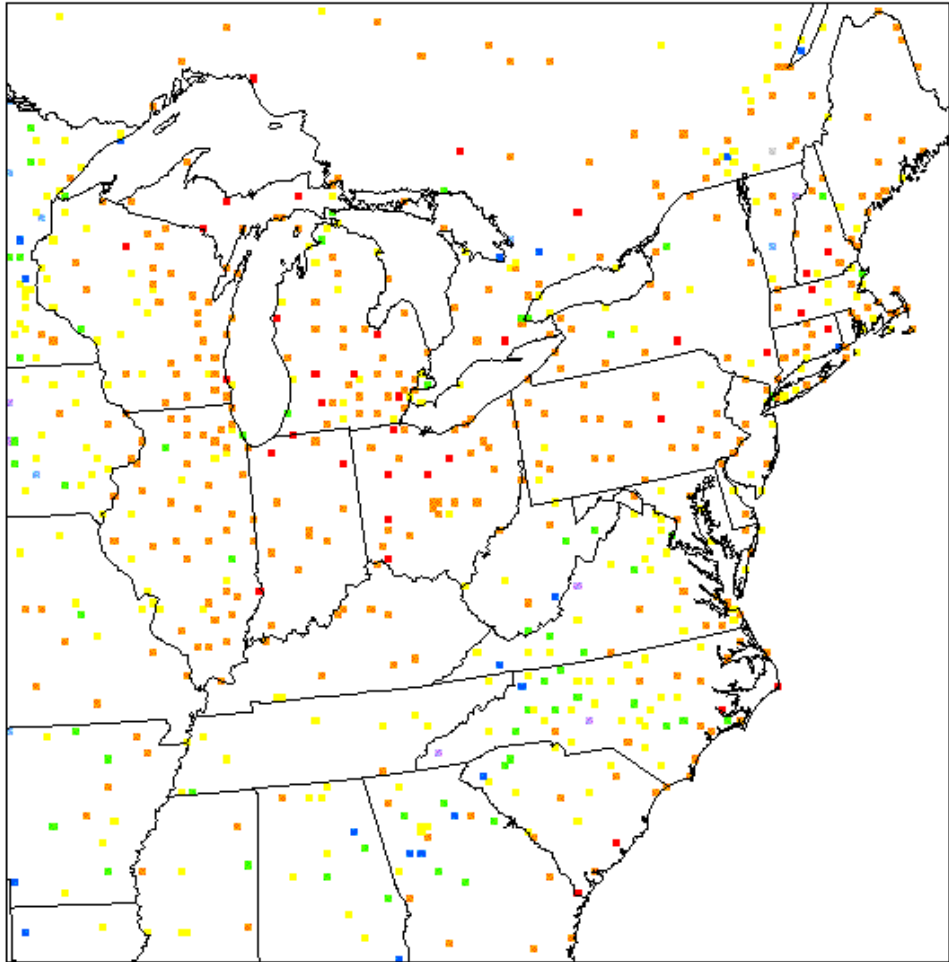


Figure 7b Spatial Correlation – Wind Speed – P-X & TDL

UMD 2002 MM5 FX Wind Speed Correlation with TDL

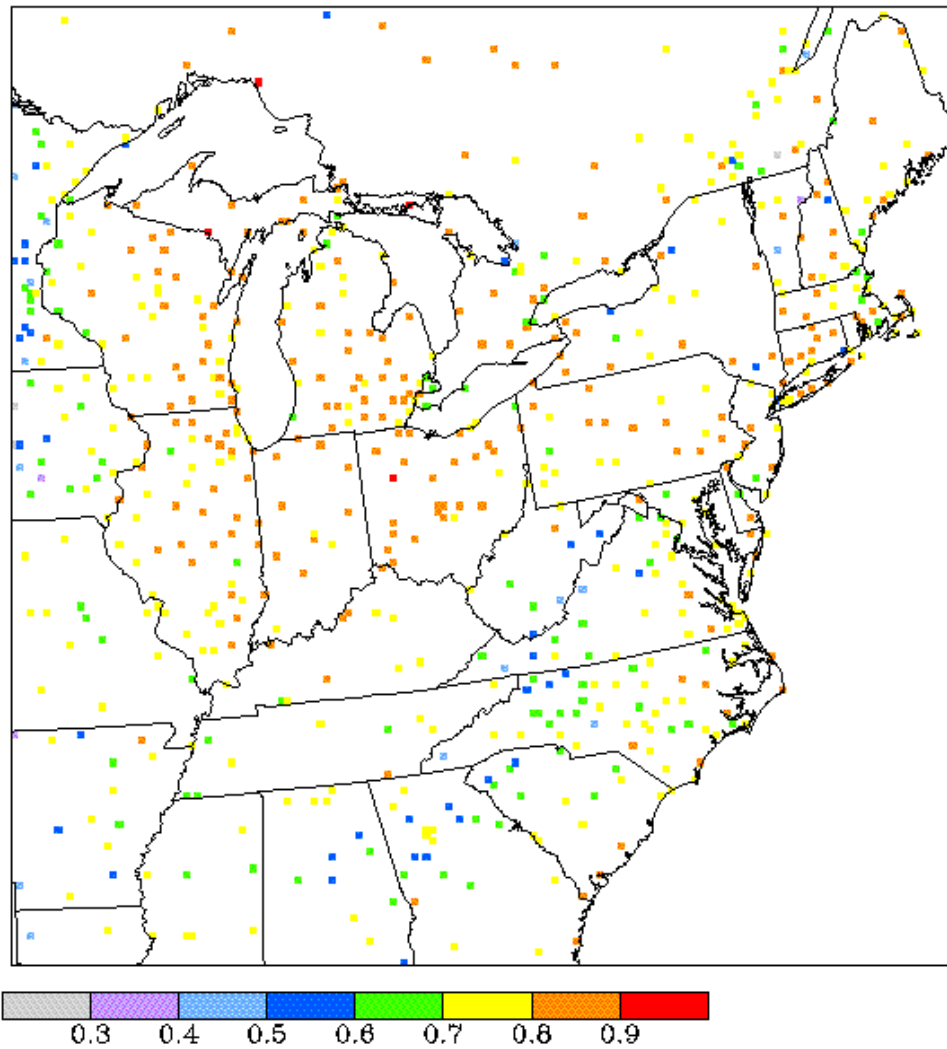


Figure 7c Spatial Correlation – Wind Speed SSiB & TDL

UMD 2002 MM5 SSiB Wind Speed Correlation with TDL

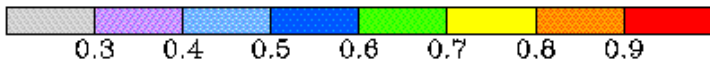
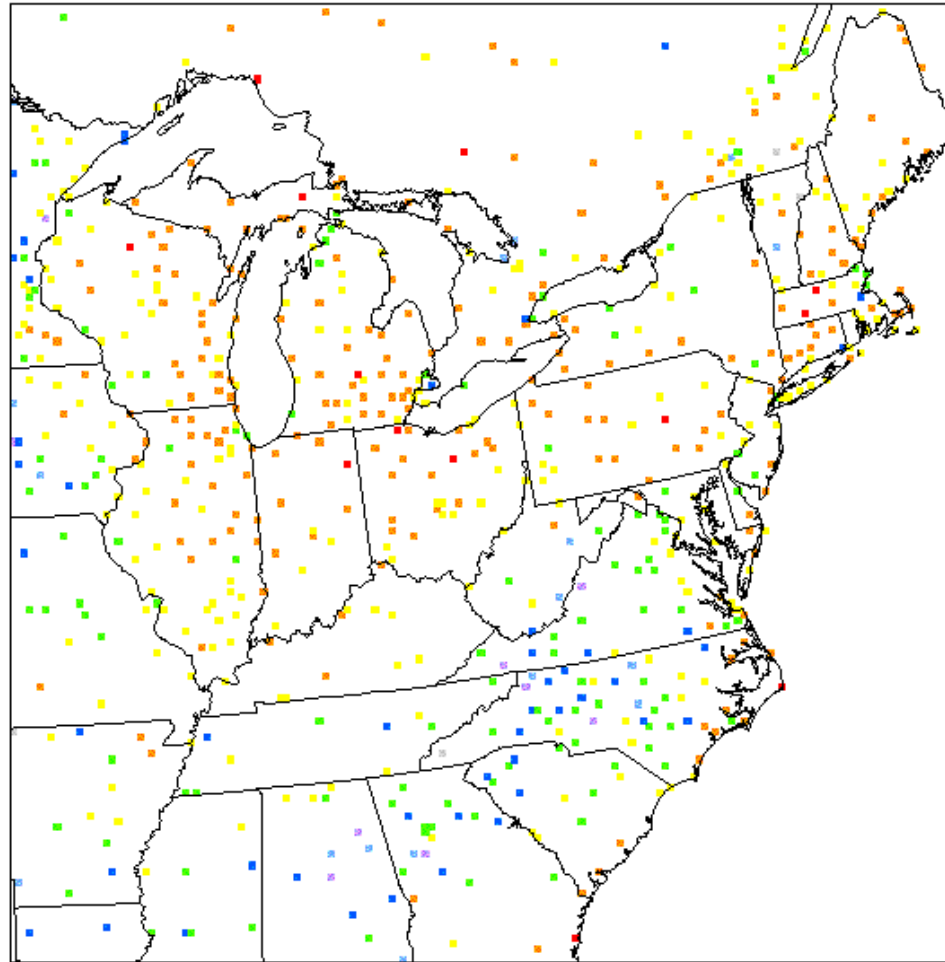


Figure 8a Spatial Correlation – Temperature – BL & TDL

UMD 2002 MM5 BL Temperature Correlation with TDL

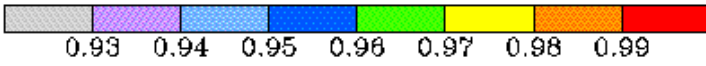
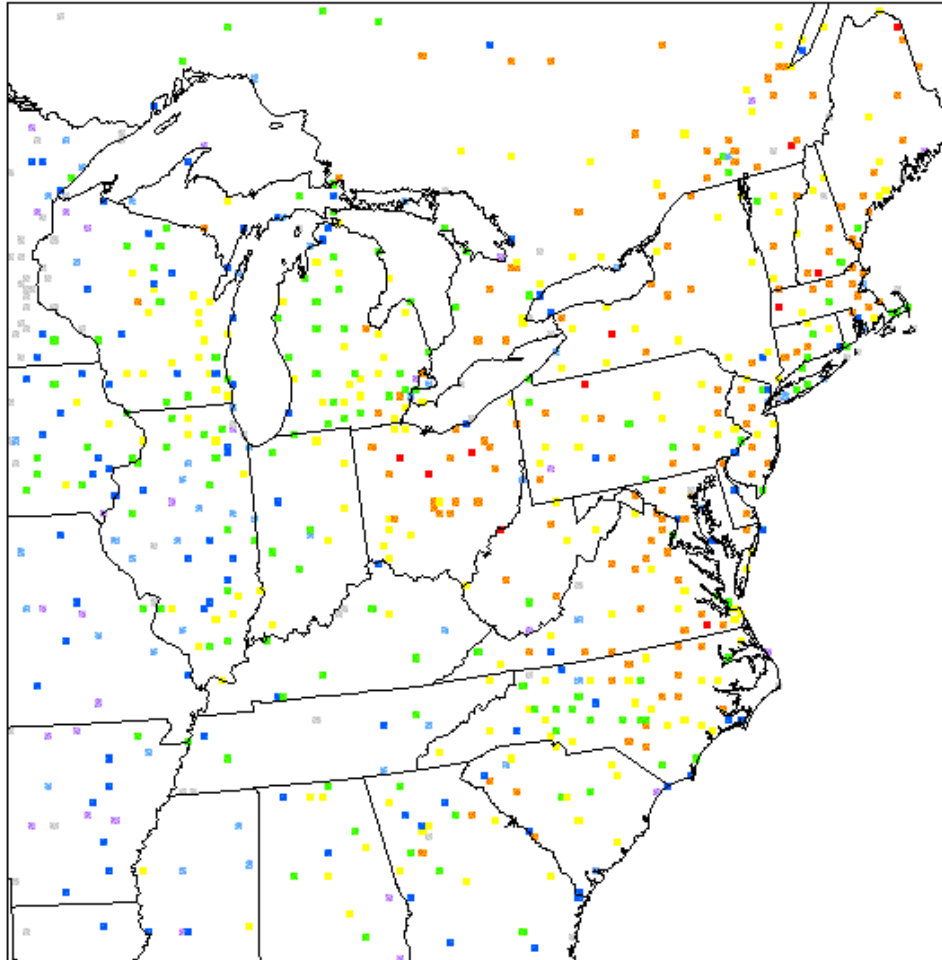


Figure 8b Spatial Correlation – Temperature – PX & TDL

UMD 2002 MM5 PX Temperature Correlation with TDL

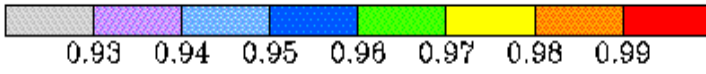
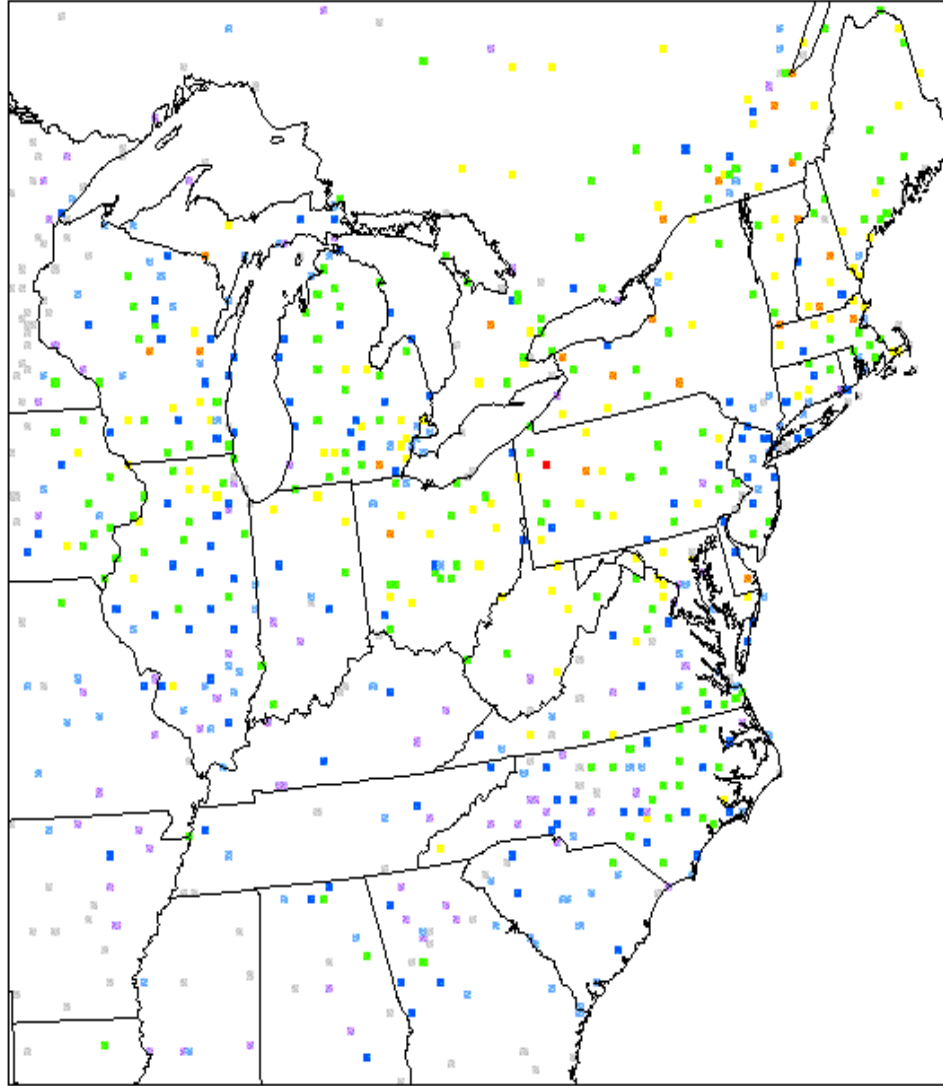


Figure 8c Spatial Correlation – Temperature SSiB & TDL

UMD 2002 MM5 SSiB Temperature Correlation with TDL

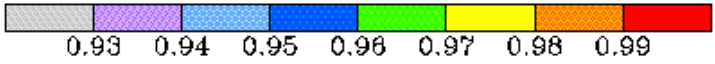
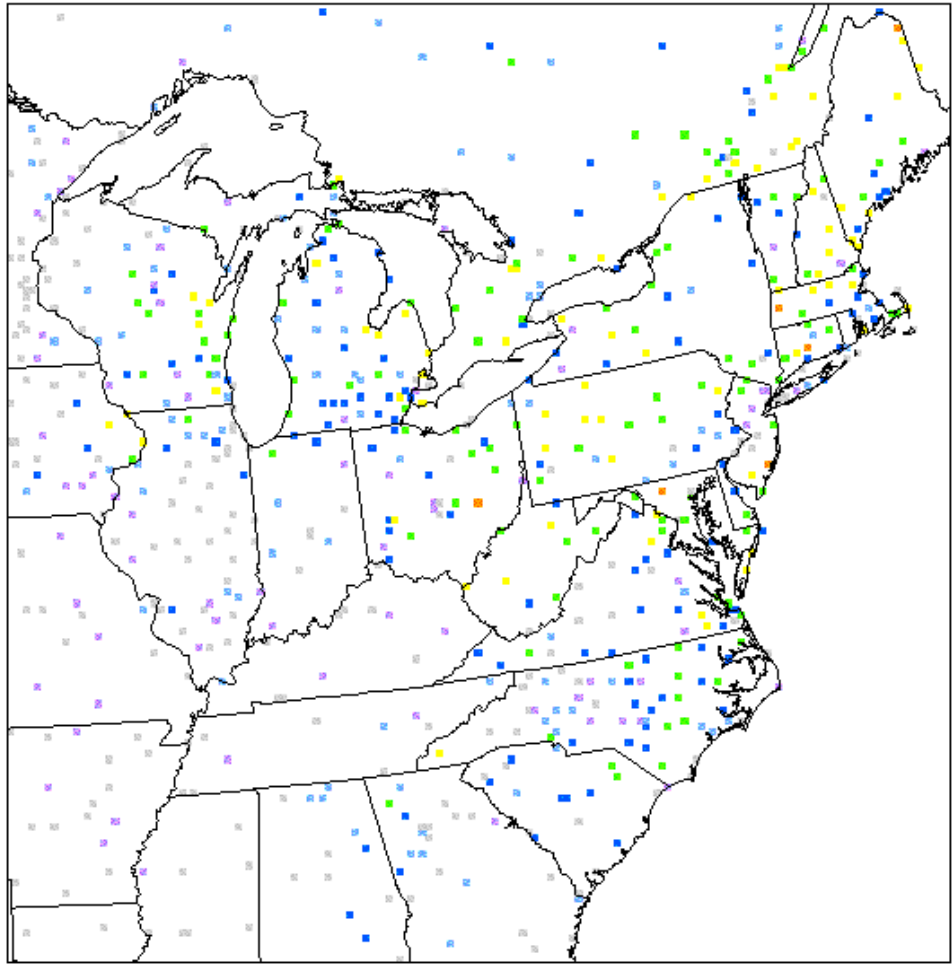


Figure 9a Spatial Correlation - Humidity BL & TDL

UMD 2002 MM5 BL Humidity Correlation with TDL

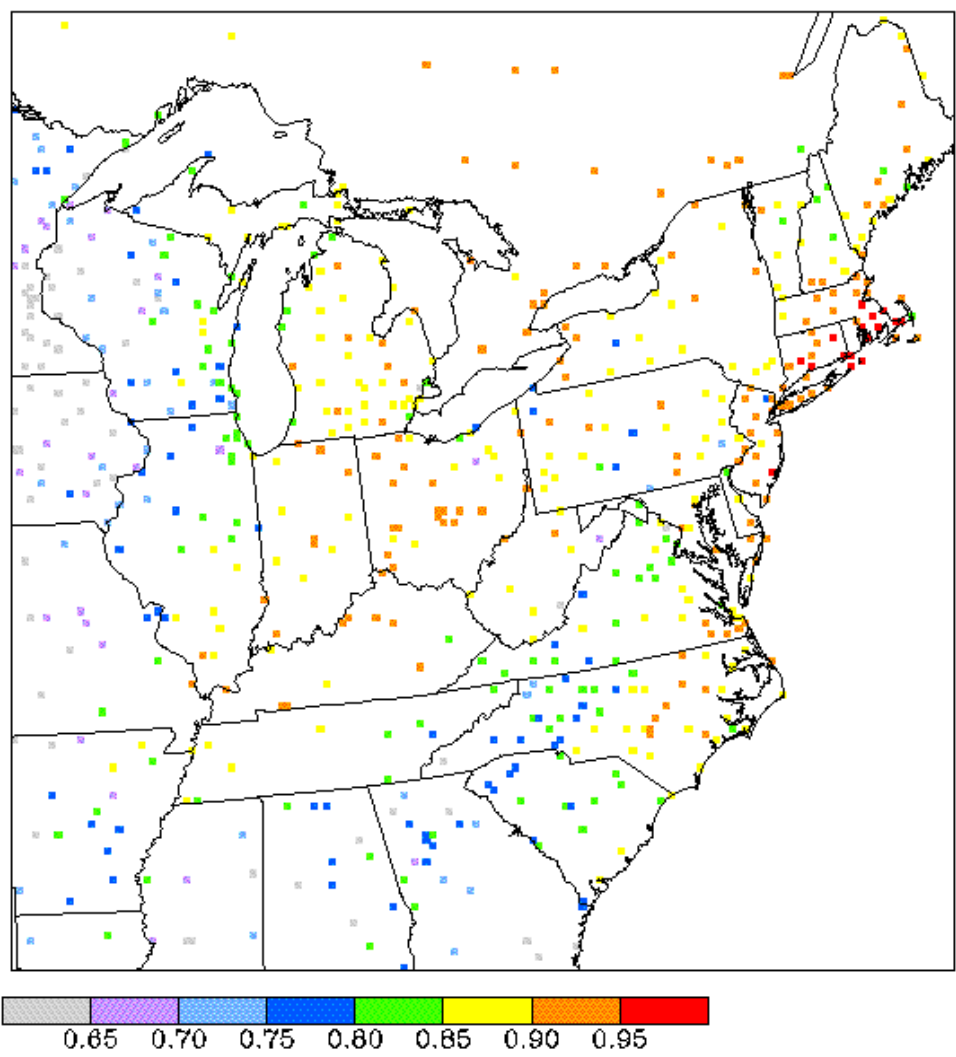


Figure 9b Spatial Correlation – Humidity PX & TDL

UMD 2002 MM5 PX Humidity Correlation with TDL

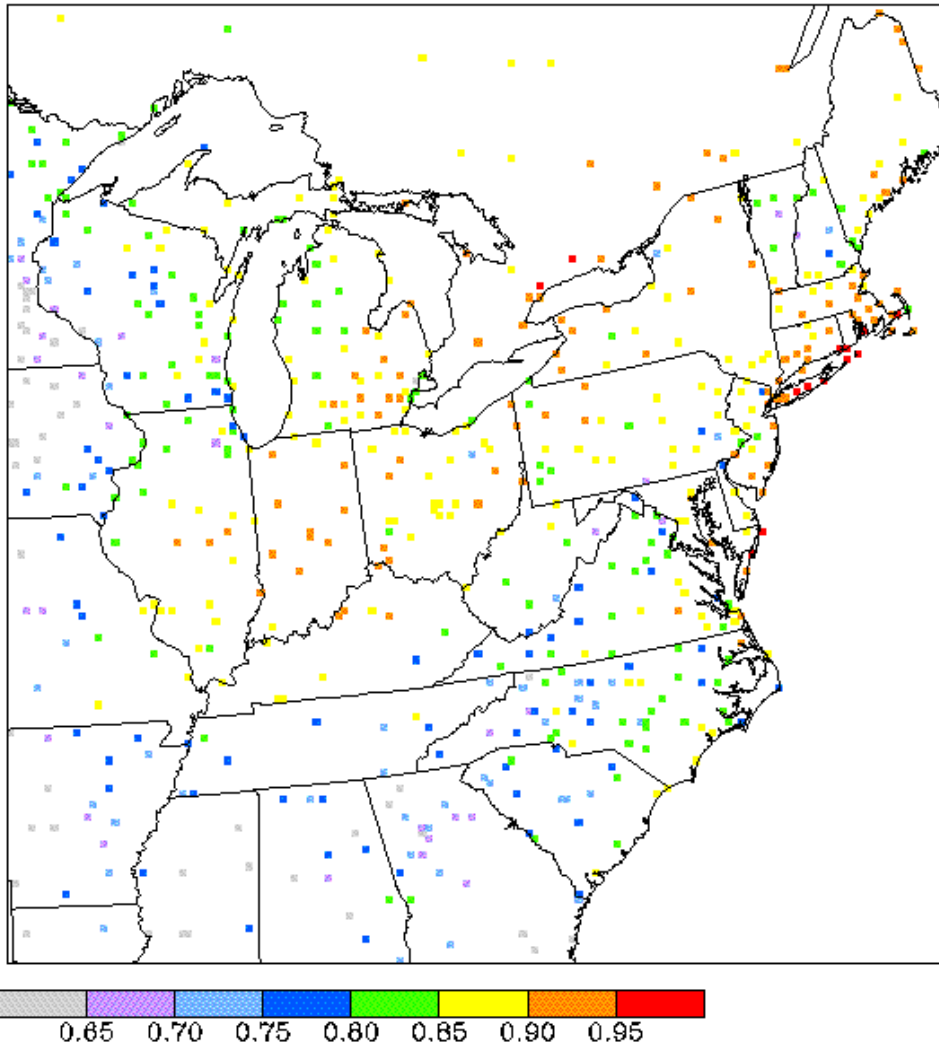
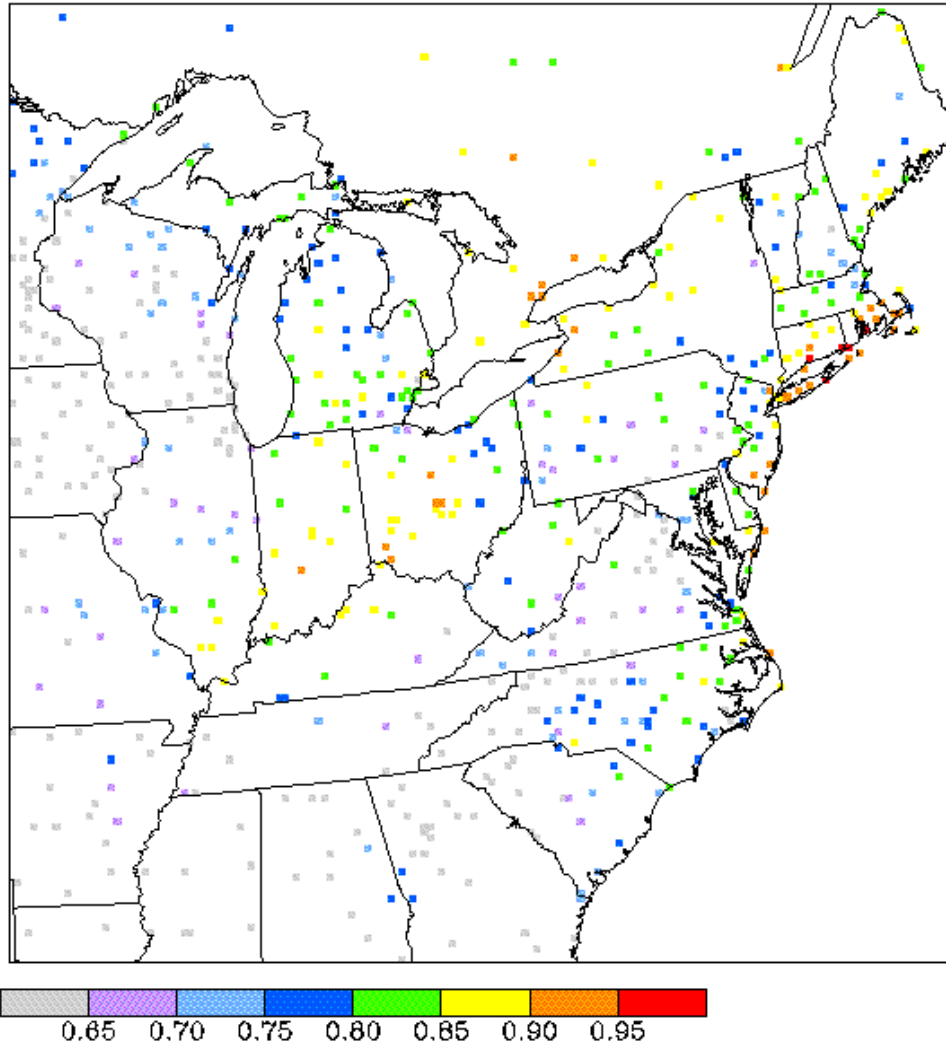


Figure 9c Spatial Correlation – Humidity SSiB & TDL

UMD 2002 MM5 SSiB Humidity Correlation with TDL



An Assessment of an MM5 Simulation of July 6 to 19, 1997, in the Eastern United States

Gopal Sistla, Mike Ku, and Winston Hao

New York State Department of Environmental Conservation

October 2002

As part of the OTC urban/regional photochemical modeling work, gridded meteorological data were simulated by the University of Maryland, College Park (UMD) with support from the Maryland State Department of Environment (MDE) using the NCAR/PSU meso-scale model MM5 version 3.3. The goals of this effort was to create a meteorological database for the summer '97 season for use with various photochemical grid models such as CMAQ, CAMx, and others to simulate and assess air quality of ozone and its precursors. The design of this MM5 modeling framework is similar to that utilized by USEPA, State of New York, State of North Carolina and others. This analysis is aimed at addressing questions such as '*how good*' are the meteorological parameters generated by MM5 when compared to the measured data. In principle such an issue should be moot given the fact that MM5 simulation utilizes observational nudging. However, in practice such a nudging is weak and is often based upon portions of the routine data measured through the National Weather Service (NWS), and therefore it is critical to undertake such a comparison with the NWS data as well as other networks that are available. In this study we undertook such an assessment of MM5 simulation covering the high ozone event of July '97 with measurements from NCAR TDL data set (ds472.0) and from the Clean Air Status and Trends Network (CASTNet). The results suggest that there may be a need for further research and improvements in exercising MM5 for air quality related applications.

Model Design

The MM5 design consists of 2-nested grids at 36 and 12 km horizontal grid resolution projected on Lambert Conformal Coordinate (LCC) system with the grid centered at 40N and 90W and the parallels at 30 and 60N. The vertical structure comprised of 25 layers and extending up to 50 mb or about 20km, with 8 levels below 1500 m. Details of the model setup are provided at ftp://www.state.ny.us/air_research/htdocs/mm5-umd-setup.htm.

Model Simulation

The simulations were performed with a 'modified' Blackadar PBL scheme and standard nudging process. The nudging data comprised of the analysis fields enhanced with observed wind field and temperature data taken from the NCEP's ADP and NCAR's NWS/TDL network. The details are provided in the attachment (Zheng 2002). The model simulations were conducted in steps of three and half days with the initial 12h considered as ramp-up time for a total of five periods covering July 6 to 19.

The success of a simulation is often assessed by its ability to reproduce observed variables, and in this case we restricted to the surface meteorological data, as they are available much more frequently, every hour, compared to the upper air measurements which are about 12 h apart. A series of tests were performed to select a PBL scheme following the determination that the existing PBL schemes in MM5 did not yield consistent surface wind speed diurnal variation compared to the observations (Ku 2002). This has led to the use of a modified Blackadar PBL scheme

(Zhang 2002)

Model Assessment

The data base for this assessment comprised of measured hourly wind speed and direction, temperature, available from two networks, viz, NCAR's NWS/TDL archive ds472.0 with stations that are often located near urban areas, and CASTNet with sites that are mostly located in rural areas (<http://www.epa.gov/castnet>). The MM5 data for this analysis were simulated at 12 km horizontal grid resolution corresponding to layer 1 that is set at a height of about 10m. The TDL temperature and wind measurements were at 2m and 10m height, respectively, while in the case of CASTNet the temperature and wind are hourly averages, measured at 9m and 10m, respectively. In this assessment the MM5 grid values were bi-linearly interpolated to the monitor location in the horizontal from the four surrounding grids, while no such interpolation was performed in the vertical. The data were processed and statistical parameters were estimated using METSTAT, a processor available with CAMx at <ftp://ftp.environ.org>.

Comparison with TDL data

Figures 1 to 3 display the diurnal variation of the measured and predicted meteorological parameters averaged over the domain that comprised of about 700 stations in the TDL database. The statistics computed are the bias, root mean square error (RMSE), and index of agreement (IOA). Visual examination of Figure 1 shows that there is very good agreement between measured and predicted temperatures, with the index of agreement around 0.9 or better. However, the bias suggests that there is a diurnally varying underprediction in the 1 to 1.5 K range during the daytime. The RMSE panel displays the systematic (RMSES) and unsystematic (RMSEU) along with the overall RMSE, which shows that the higher level of error occur during the day time than in the night time. This appears to

arise mainly from the systematic part of the error, suggesting that this perhaps can be minimized further. Note, the unsystematic error is also contributing similarly, with a maximum in the nighttime hours. The index of agreement (IOA) shows essentially a constant level around 95% or so, indicating an overall agreement between model estimates and measured surface temperatures. Figure 2 displays the statistics of wind speed and direction averaged over the domain. In general, the measured peak wind speed is higher than that predicted with a slight phase of about 1 to 2 hours the predictions lagging the observations and bias varying from 0 to -1.0m/s during the day time reaching the maximum in the afternoon time. The RMSE panel indicates that the bulk of the bias is perhaps associated with the unsystematic error (RMSEU). However, in the case of wind direction, it appears to exhibit the least bias over the simulation period. Figure 3 compares the measured and predicted humidity variable, mixing ratio, again averaged over the modeling domain. While the measured data shows a shallow morning dip and an afternoon rise followed by a shallow dip and rise towards the end of the day, the predicted data often exhibits an afternoon minimum for each day. This is reflected in the bias with the underprediction exhibiting a maximum around mid-day by as much as 3.0g/kg. The RMSE panel also shows the same feature with the systematic error contributing major portion of the underprediction.

The above comparison of the TDL data does not provide any information as to how the model has fared spatially over the domain. This was accomplished by examining the level of correlation at each monitor for the three meteorological parameters and the spatial correlation are displayed in Figures 4 through 6. In the case of temperature, the correlation is quite high (>0.9) (see Figure 4) and visual examination shows that there is no geographical bias. In the case of wind speed, the correlation values exhibit a wide range (see Figure 5) with some of the monitors at <0.3 . It also appears that there is some tendency towards higher degree of correlation in the upper half of the domain compared to the lower half. Figure 6 displays the correlation across the domain for the mixing ratio (humidity) parameter, which also vary from <0.3 to >0.9 , and exhibit a distinct geographical demarcation with higher correlation values being associated with monitors in the upper-half of the domain.

Comparison with CASTNet data

Similar to the TDL analysis, Figures 7 and 8 display domain averaged diurnal for measured and predicted temperature, wind speed and direction based on about 50 monitoring sites. Since there is no measured station pressure, mixing ratios were not calculated, even though relative humidity is available at these monitors. The

statistical parameters considered are bias, root mean square error (RMSE) and index of agreement (IOA), which were computed using the METSTAT program, as before. In the case of temperature (see Figure 7) while the observed and predicted diurnal average temperature exhibits a good agreement, the bias was found to vary from -1 to 2.5K with over prediction in the late afternoon and under prediction during early morning hours. This is in opposite direction to the TDL comparison. Examining the RMSE panel shows that the RMSE is higher during the late afternoons coincident with the over prediction and is comprised mostly of systematic error (RMSES). This feature that the error is arising from systematic error portion of the RMSE is consistent with that of the TDL comparison, but the time of occurrence of the maximum error differs between the two data sets. The index of agreement (IOA) for temperature is around 0.9 for most portions of the simulation, indicating that the model performs quite well for this parameter. Examining Figure 8 shows that the predicted wind speeds are generally higher than the measured speed by about 0.5 to 1 m/s with the measured peak occurring in advance of the model predicted maximum. Examining the bias, exhibits the over prediction of the maximum, diametrically different from the comparison of the TDL data (see Figure 2). The RMSE panel exhibits the systematic (RMSES) and unsystematic (RMSEU) errors, with the systematic error generally in the less than 1.5 m/s. The index of agreement (IOA) for wind speed is in fair agreement averaging about 0.7, quite similar to the comparison with the TDL data. Examining the wind direction panels show that the results are similar to those of TDL data.

We have also examined on a spatial basis the level of correlation at each of these monitors and are displayed in Figures 9 and 10 for temperature and wind speed, respectively. While the distribution of the monitors is not as spatially intensive as that of TDL, a high degree of correlation, > 0.9 , is found for the temperature. However, in the case of wind speed the level of correlation is considerably lower and varies over the domain, similar to that of TDL (see Figure 5). Also, there appears to be slightly higher level of correlation in the upper-half of the domain compared to the lower-half.

On an overall basis, the CASTNet data exhibit slightly lower correlation than the TDL data set which is not unexpected since the former were not part of the data base used for nudging.

Discussion

The comparisons performed in this study are unique in that the comparison is made both with measured data from

TDL that had been used to do observational nudging and with data taken from CASTNet that were not part of the nudging. The qualitative results show that the model predictions are quite similar for both sets of data, and in terms of spatial correlation the model tends to exhibit slightly better correspondence for wind speed over portions of the upper-half of the domain than in the lower-half. In the case of mixing ratio (relative humidity), the model appears to capture the early morning dip, but fails to exhibit the mid-morning rise seen in the observed data, but apparently tracks fairly well the over-all pattern of increasing trend observed during this period. These comparisons show, that the MM5 simulation for surface temperature, wind speed and direction are comparable with measured data, and perhaps could be strengthened with other additional assessments.

Other comparisons and issues

Additional assessments that can be performed but were not included in this study are the cloud cover and precipitation. In the case of the former, comparison can be performed indirectly between ground level photo-synthetically activated radiation (PAR) derived from satellite images and that estimated from the MM5 simulation. In the case of precipitation, the comparison can be performed between NCAR archive ds505.0 consisting of hourly data to that predicted by MM5. It is anticipated that with these types of additional comparisons between predicted and measured data, it perhaps would be possible to reach a better decision on the ability of MM5 to simulate the observed meteorological parameters which are critical for air quality simulation effort. In addition we would like to note that in some instances there are sharp spatial gradients between the computed mixing heights, especially during the non-daylight hours. An example of this is displayed in Figure 11 indicating the estimated mixing heights at about 2200 EST. While we had not yet investigated the cause of these excursions, it is important to develop and apply diagnostic tools for achieving better meteorological fields for application in air pollution problems.

In Figure 12, we display the composite and average observed and predicted diurnal cycles of the water vapor mixing ratio based upon the seasonal (June, July, August, 1995) simulation using RAMS and MM5 at a grid spacing of 36km covering the eastern United States (Hogrefe 2002). It is interesting to note that both models are found to predict the observed double peak structure, suggesting that there is a need for further assessment of this problem.

Next Steps

The meteorological data are being processed to develop inputs to the photochemical models. The issues such as the mixing height, mixing ratio, require further diagnosing of the model. The problem with the mixing ratio of water vapor appears to extend to other prognostic model RAMS as well, suggesting the need for careful assessment of the codes. While these are critical components for developing reliable meteorological fields, their role on the estimated air quality needs further assessment as exercises are undertaken with the 'improving' meteorological inputs in application of photochemical models.

References

Hogrefe, C (2002) Private communication

Ku, M., et al. (2002) Presentation at the AMS, AWMA Joint meeting at Virginia Beach, VA.

Zhang, Dalin (2002) Presentation to MDE, Baltimore, MD

Zheng, W (2002) See attached

Attachment

Numerical Simulations of the Ozone Episodes of 5 - 20 July 1997

Weizhong Zheng, Department of Meteorology, University of Maryland at College Park, College Park, MD

The MM5 simulations were started from 1200 UTC July 5 to 0000 UTC 21 July 1997, and they are re-initialized every 3.5 days. The next cycle starts on day 3 of the previous cycle, providing a 12-h overlap between two consecutive cycles.

1. Model description.

The version 3.3 of MM5 is used for these simulations. The domain and vertical levels are defined the same as previously reported.

The main physical schemes used in these runs include:

- (a) The latest version of Kain-Fritsch convective scheme used for both 36- and 12-km resolution domains;
- (b) An explicit moisture scheme (without the mixed phase) containing prognostic equations for cloud water (ice) and rainwater (snow);
- (c) The Blackadar planetary boundary layer (PBL) scheme;
- (d) A simple radiative cooling scheme;
- (e) A multi-layer soil model to predict land surface temperatures using the surface energy budget equation.

The PBL schemes we tested include the following 5 schemes: the Gayno-Seaman TKE scheme, Burk-Thompson, Blackadar, MRF, and Miller-Yamada-Janjic. Only the non-local scheme of the Blackadar PBL parameterization can reproduce the right diurnal cycle of V_{sfc} , while the other schemes tend to produce too weak surface winds during the daytime and too strong surface winds near midnight. However, the original Blackadar scheme tends to show too well-mixed momentum in the PBL and too fast upward transport of moisture. After some modifications of the Blackadar scheme by changing the mass exchange between the surface layer and the layers above, the scheme is able to produce reasonable diurnal cycle of V_{sfc} , T_{sfc} and surface relative humidity. These changes are given as follows

- (a) The K-coefficient is determined by the Richardson number according to Zhang & Anthes (1982), where the critical Richardson number is set to be 0.25 rather than to be calculated with Shir and Bornstein method (1977). And the length l is set to be depth of the model layer.
- (b) Using potential temperature rather than virtual potential temperature to calculate the bulk Richardson number R_b .
- (c) Weighting function is used not only for momentum but also for potential temperature and mixing ratio.

2. Nudging Processes

The dynamical nudging is used for each domain. The observed upper-air wind, temperature and mixing ratio fields are nudged every 6 h, while the surface wind and temperature field are nudged every 3 h, but the temperature (except for at the surface) and the mixing ratio field is excluded the PBL nudging.

3. Model initialization

The model is initialized by using NCEP's Eta model analysis as a first guess that is then enhanced by observations at the upper levels and the surface.

- (a) NCEP's ADP global upper-air observations (NCAR archive ds353.4) are used to further enhance the upper-level Eta analysis.
- (b) The following two sets of surface observations have been introduced into the model initialization to improve the Eta analysis of surface winds and surface temperature fields:
 - NCEP's ADP global surface wind observations (NCAR archive ds 464.0). This dataset provides 6-hourly surface observations over land in one stream, and 3-hourly over both land and ocean surfaces in another stream.
 - NWS/TDL's U.S. and Canadian surface observations (NCAR archive ds472.0). This dataset provides hourly surface observations over the U.S. and Canadian regions.

The Cressman objective analyses option is used to enhance the Eta analysis. However, we analyzed the results and found that it still could not reproduce the right diurnal cycle of V_{sfc} and T_{sfc} . Thus, we repeat the Cressman procedures three times more to enhance the surface analyses. Results indicate that this procedure significantly improves the results.

Figure 1 Comparison of TDL observed and MM5 predicted temperatures for July 6 to 19, 1997

MM5 Simulation by UMD (revised)

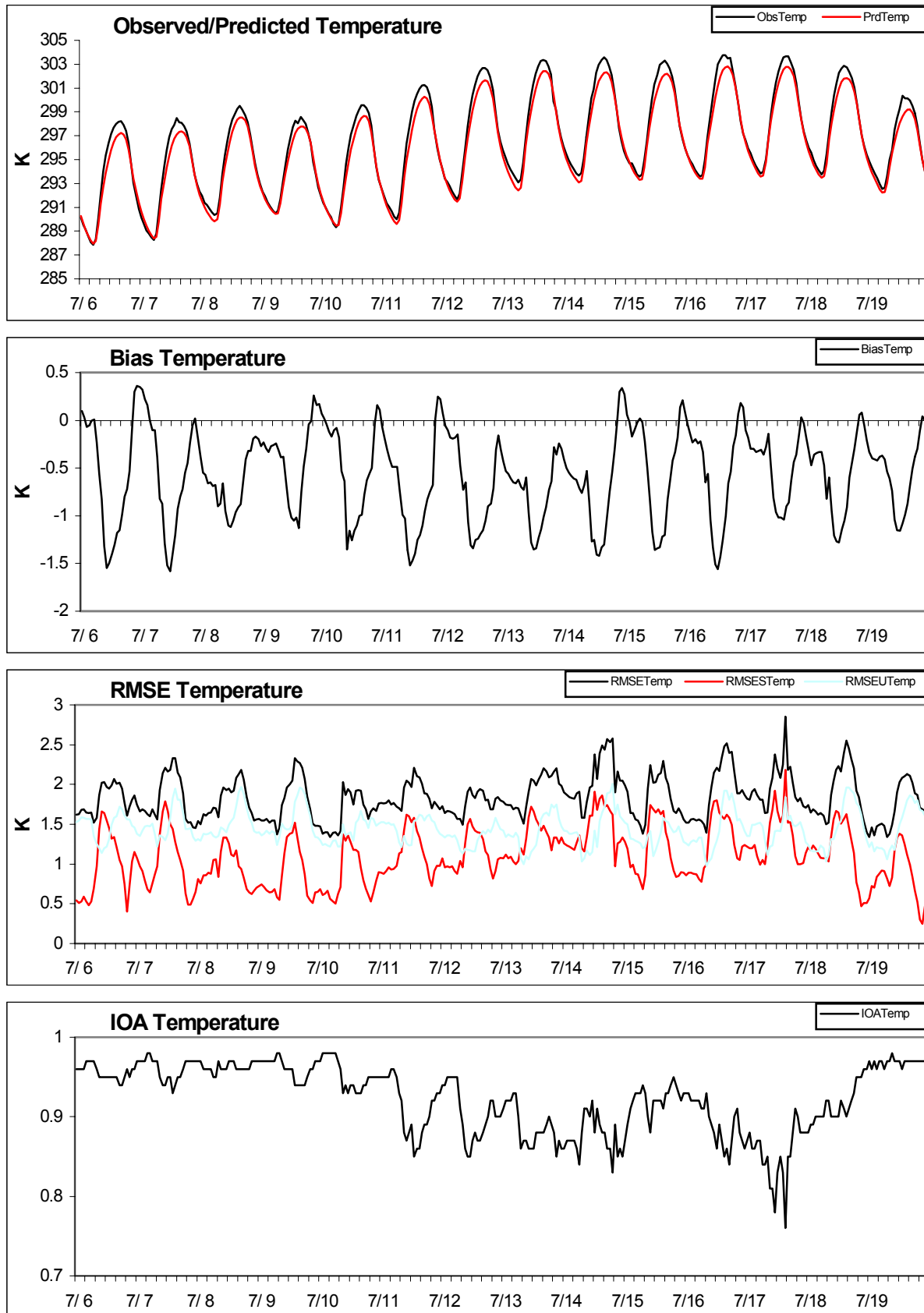


Figure 2 MM5 Predicted and TDL measured ws and wd, July 6 to 19, 1997
MM5 Simulation by UMD (revised)

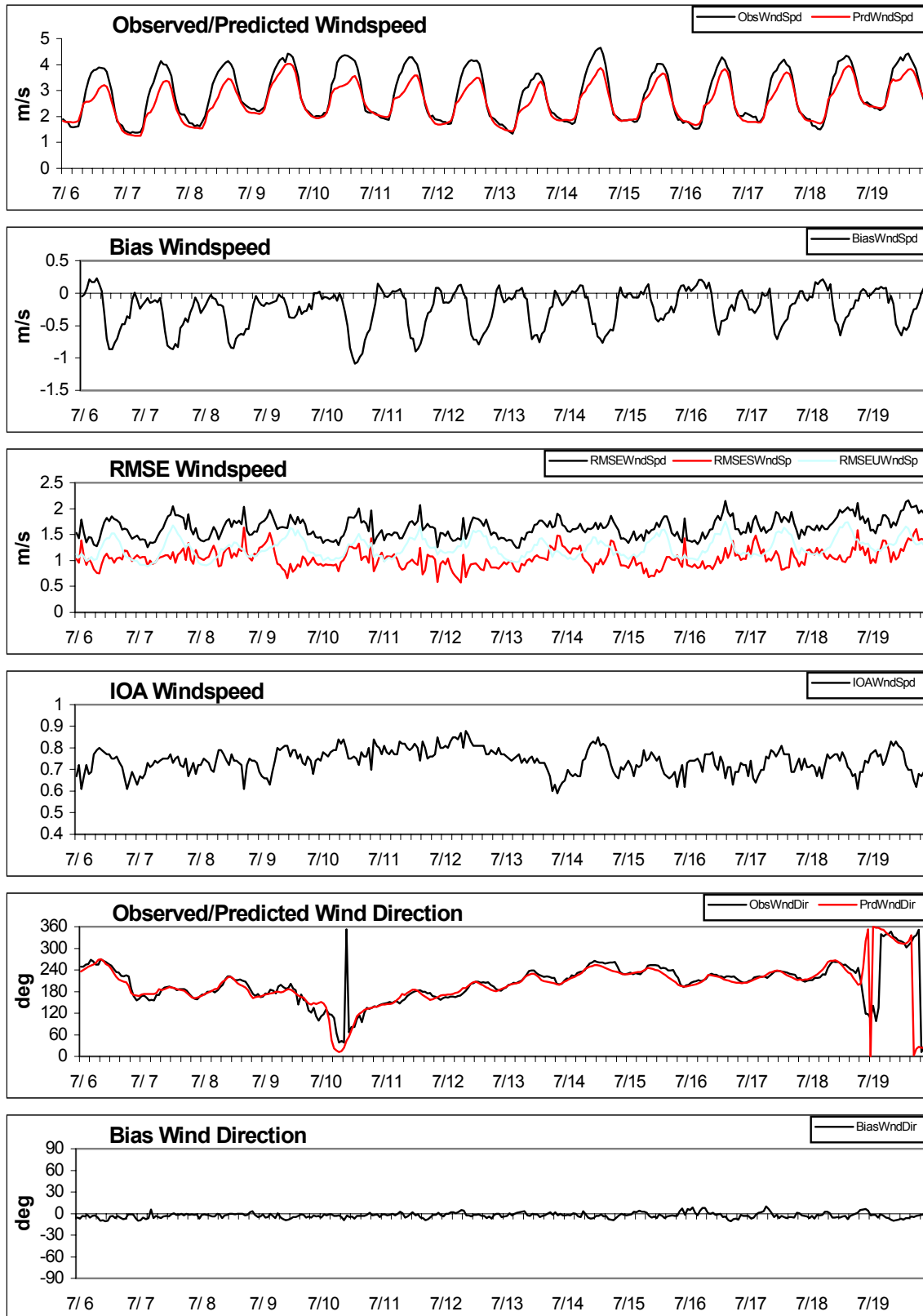


Figure 3 MM5 Predicted and TDL measured mixing ratio (humidity) for July 6 to 19, 1997

MM5 Simulation by UMD (revised)

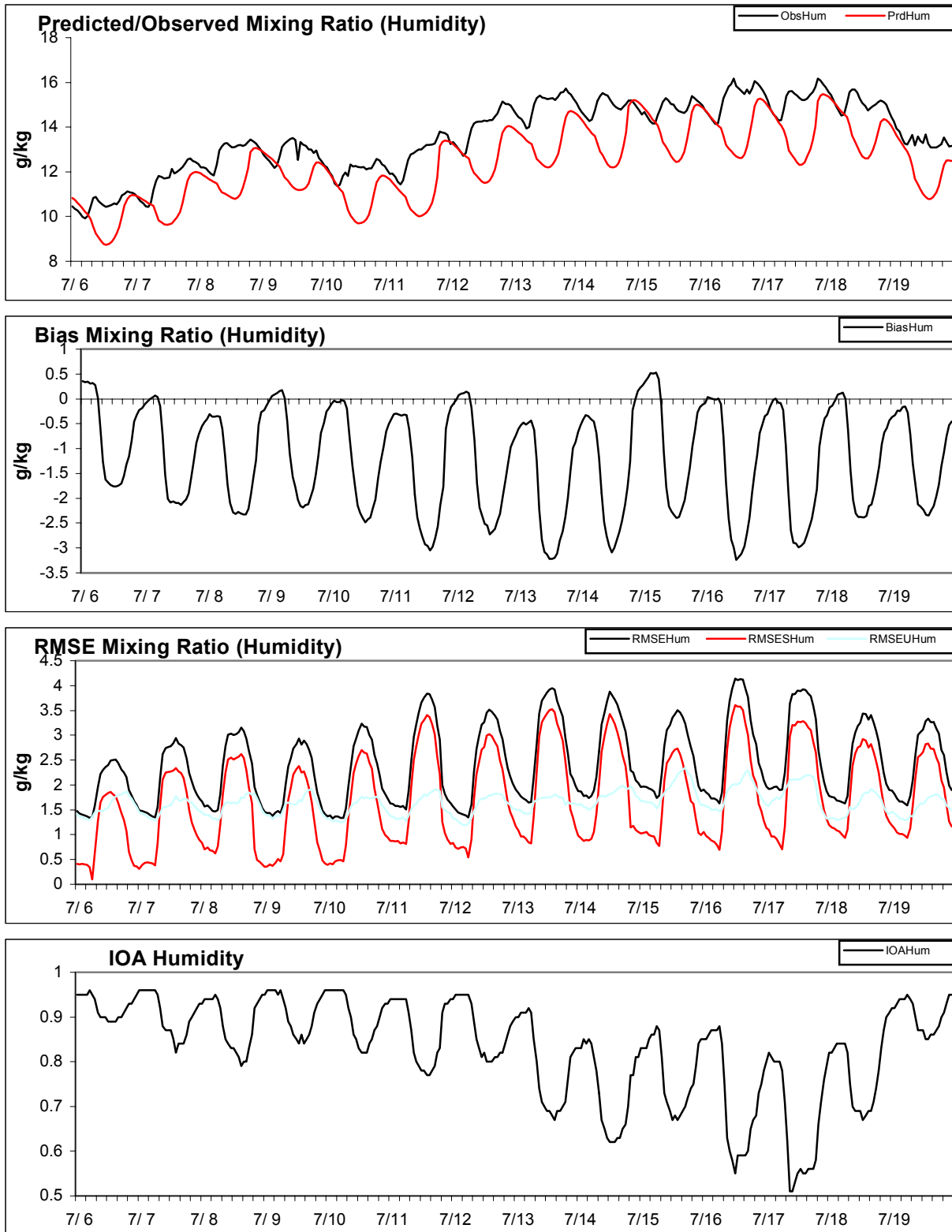


Figure 4

Correlation between MM5 Predicted and TDL-based
Temperatures for July 6 to 19, 1997

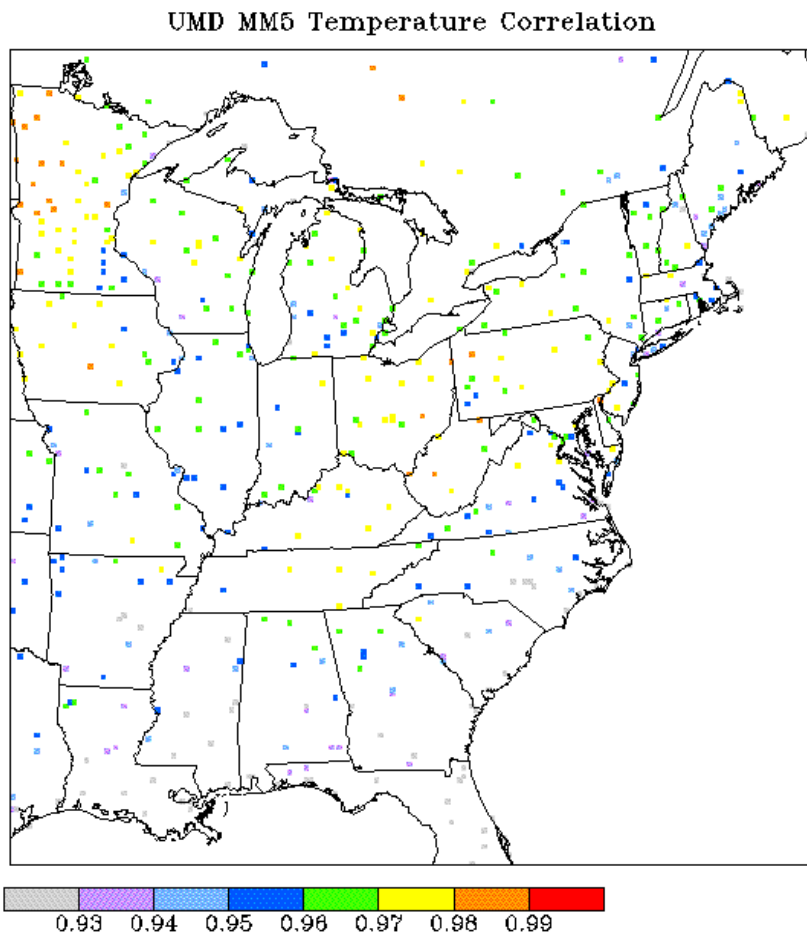


Figure 5 Correlation between MM5 Predicted and TDL-based wind speeds for July 6 to 19, 1997

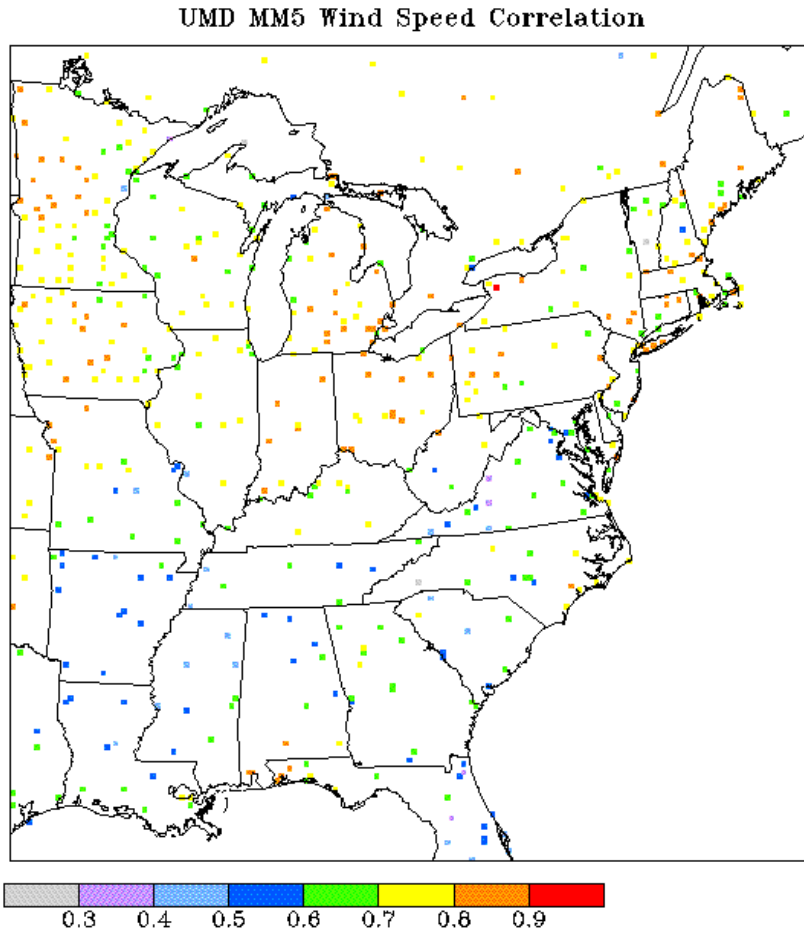


Figure 6

Correlation between MM5 Predicted and TDL-based mixing ratio (humidity) for July 6 to 19, 1997

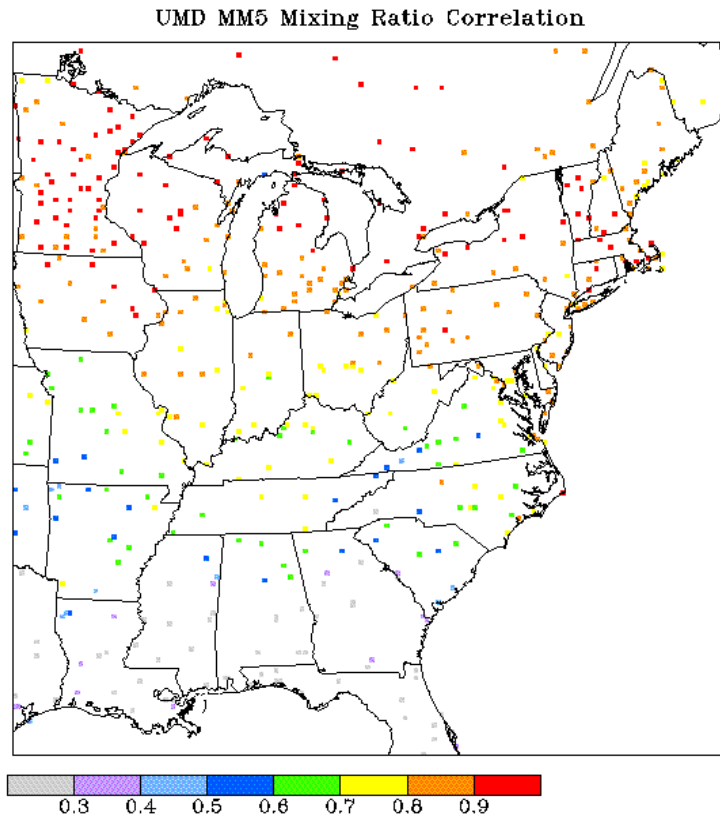
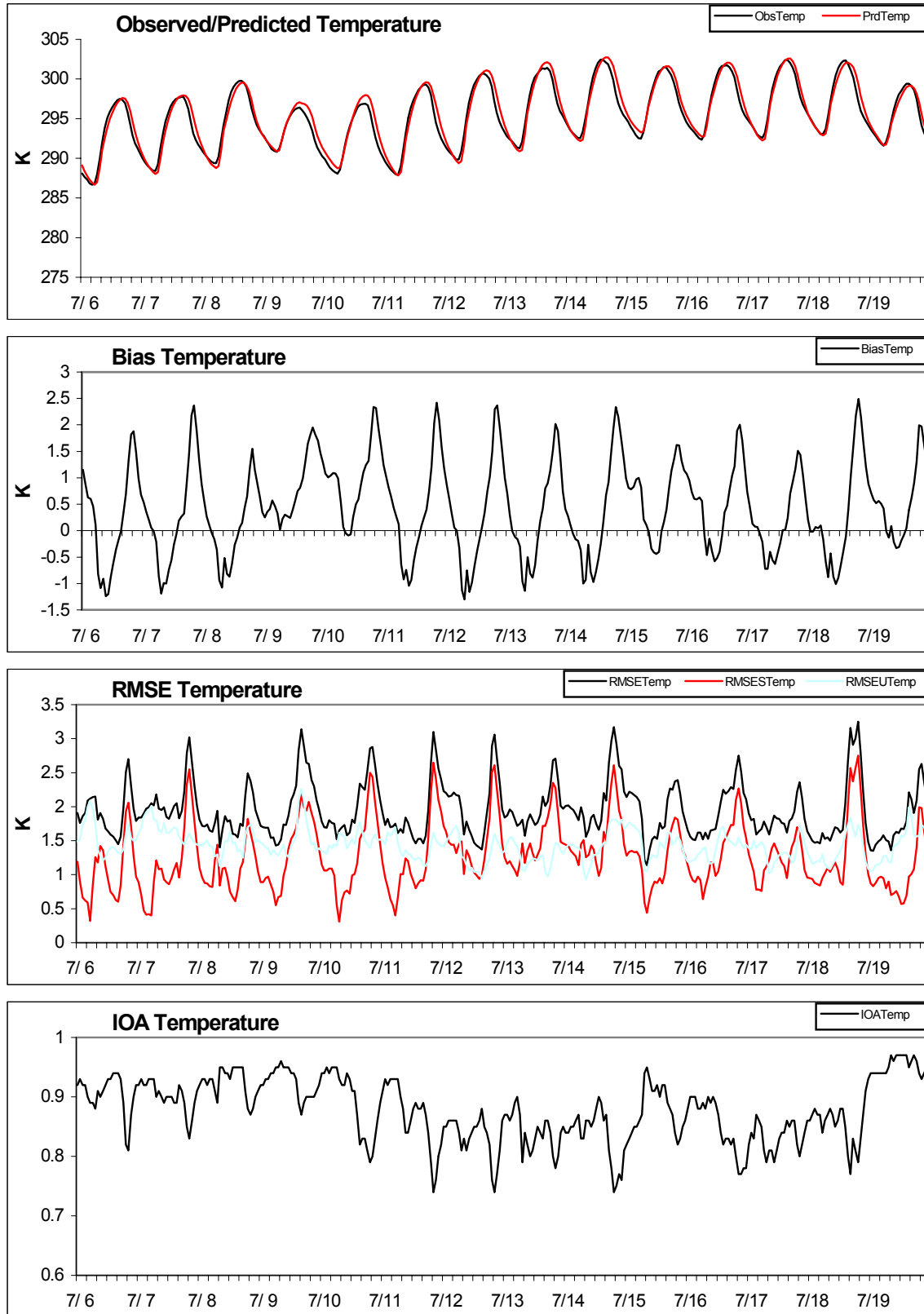
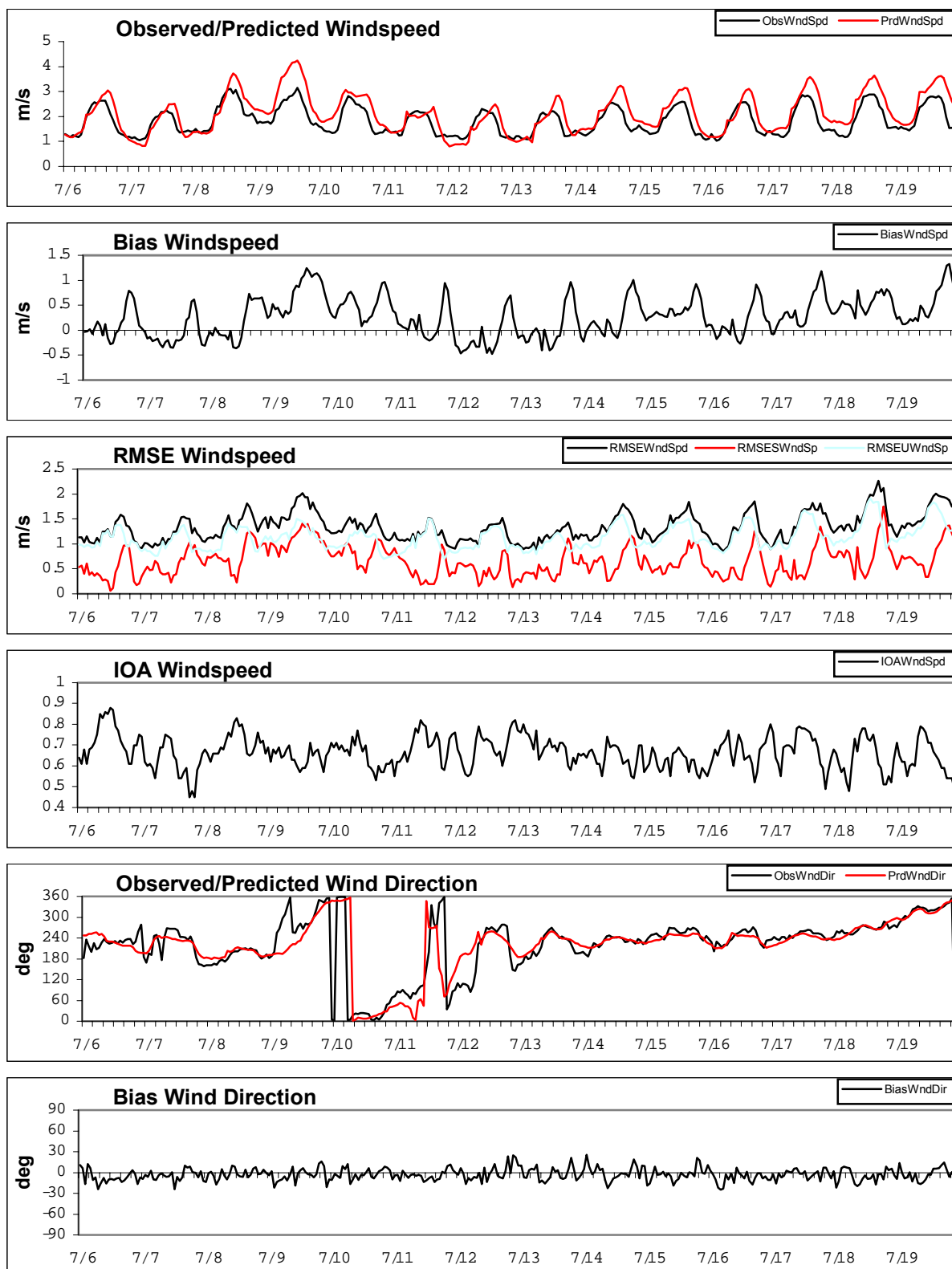
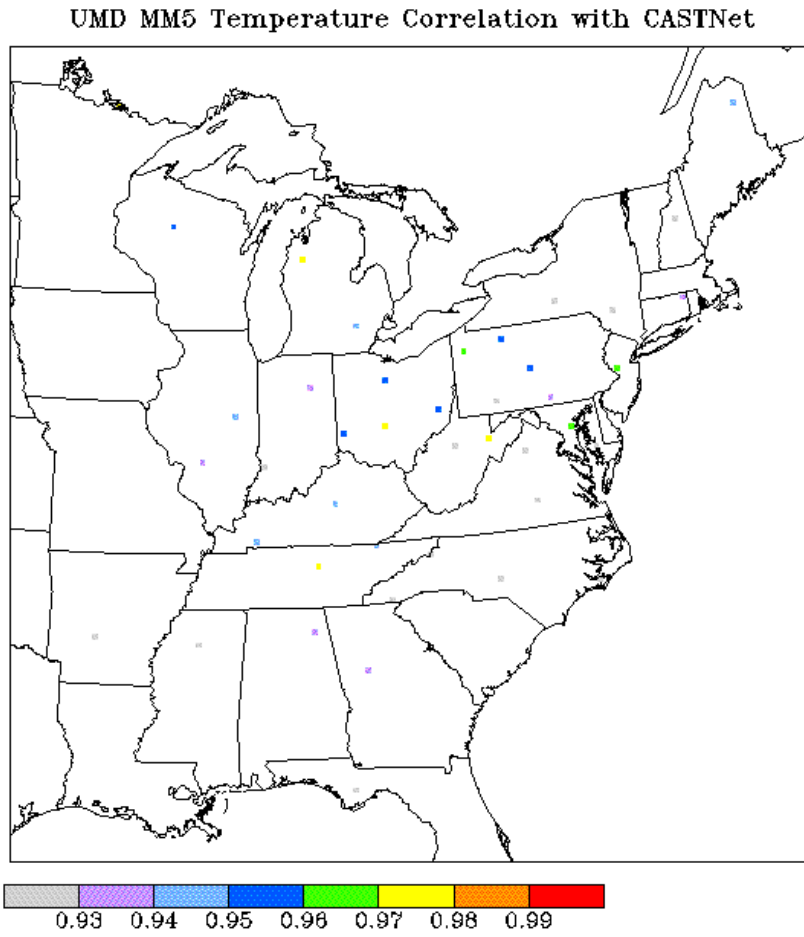


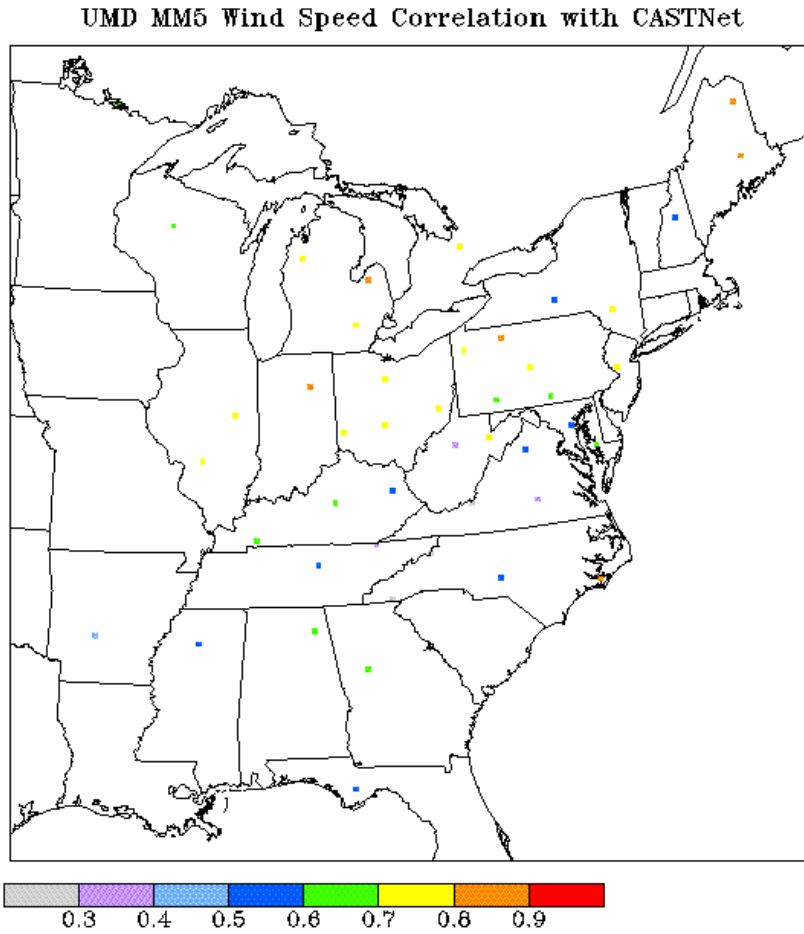
Figure 7 MM5 Predicted and CASTNet measured temperatures, July 6 to 19, 1997
MM5 Simulation by UMD (revised) July 6 to 19 1997 vs CASTNet



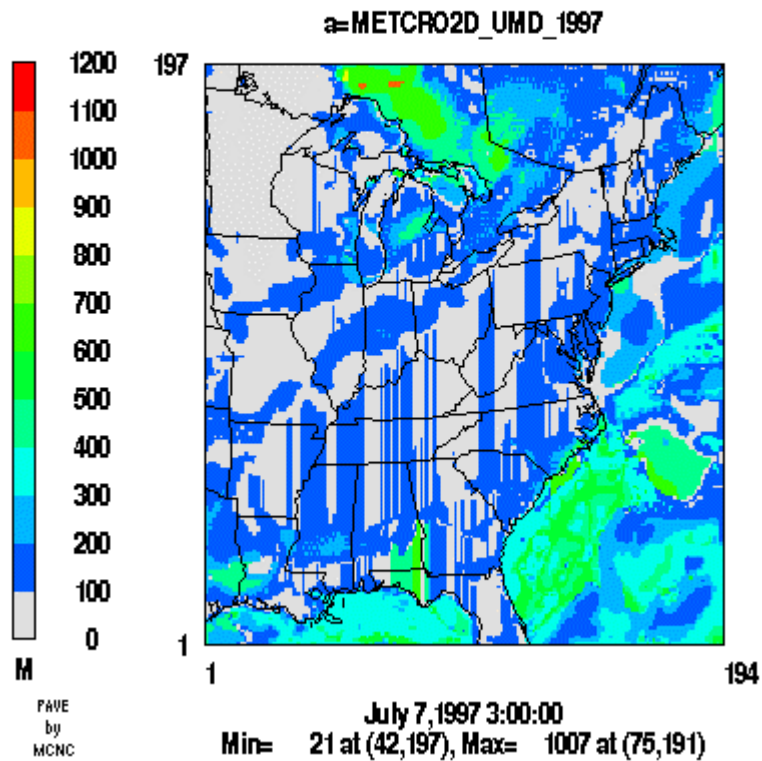
**Figure 8 MM5 Predicted and CASTNet measured ws and wd for July 6 to 19, 2007
MM5 Simulation by UMD (revised) July 6 to 19 1997 vs CASTNet**



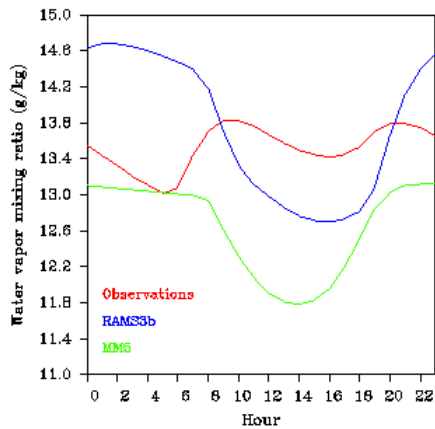




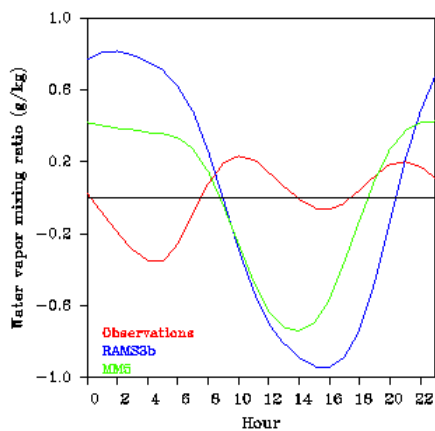
Layer 1 PBLa



Composite diurnal cycles of observed and predicted Water vapor mixing ratio, spatial and temporal average



Average cycles of observed and predicted diurnal components Water vapor mixing ratio, spatial and temporal average



Further comparison of MM5 simulations for the July 11 to 15, 1997 period

The MCNC Environmental group using MM5 has simulated the July 1997 high ozone episode. The results of their analysis were posted at <http://www.emc.mcnc.org/projects/NCDAQ/Met/97e>. The design and exercising of the MM5 model by this group differs from that of UMD (see ftp://www.dec.state.ny.us/dar/air_research/htdocs/mm5-umd-setup.htm) even though the definition of the projection of the grid is the same between the two simulations.

Some of the salient differences are: vertical grid structure; areal extent of the grids; and the shorter period of simulation [July 10 (12Z) to July 16 (12Z) 1997 of MCNC compared to July 5 (12Z) to July 21(00Z), 1997 by UMD]. Details of the setup can be found at the above referenced URLs. In this analysis, we focus on the relative response of the two simulations over the common region of the 12km grid to the TDL and CASTNet measurements. To this end, we obtained the gridded data for the MCNC run identified as Case E. The 12 km grid, identified as D02, covers portions of VA, WV, KY, TN, GA, SC besides NC and is shown in Figure 1, adapted from the MCNC web site. Briefly, the UMD simulation consists of 2-way nested 36/12 km grid, while the MCNC utilized 3grids at 36/12/4 km one-way nesting. The comparison is made between D02, the area shown in Figure 1 of the MCNC domain to the corresponding portion of the UMD domain (see Figure2). The statistical measures were developed using the METSTAT from Environ (see <ftp://camx.pass4camx@ftp.environ.org/processors/metstat.24jan02tar.z>).

TDL data comparison

Figure 3 and 4 display the comparison of the MM5 predictions to measured wind speed, that were part of the TDL data utilized in the nudging for MCNC and UMD simulations, respectively. The MCNC estimates of wind speed exhibit both over and under prediction, while the UMD estimate shows under prediction of the measured wind speeds. While the under prediction in both cases is associated with the peak wind speed, the MCNC data shows over prediction for the hours with minimum wind speed as well unlike the UMD data. The wind direction on the other hand shows very good agreement with both models and bias that is generally near the zero line.

Figures 5 and 6 display the comparison of the predicted temperatures from MCNC and UMD to that measured under TDL, respectively. Both models show good agreement to the TDL data, with the UMD data exhibiting slightly lower bias than the MCNC simulation. The bias range for UMD is from 0.5 to -2.5 C, while for MCNC it ranges from 1.5 to -4 C.

Figures 7 and 8 display the comparison of the predicted and measured mixing ratio based on MCNC and UMD simulations, respectively. In general, both simulations tend to under predict with the UMD estimates showing an occasional agreement with the measured data. However, the diurnal variation appears to show a better match visually with observations for the MCNC simulation.

CASTNet data comparison

Figures 9 and 10 display the average observed and predicted wind speed and direction for MCNC and UMD simulations, respectively for the common 12 km domain. The average wind speeds measured at the CASTNet sites are in the 1 to 2m/s range compared to the TDL sites which range from 1 to 4 m/s. The MCNC simulation exhibits generally a positive bias, while the UMD shows a negative bias, in both cases as high as 1m/s.

Figure 11 and 12 display the average observed and predicted temperatures based on MCNC and UMD simulations, respectively. While the MCNC simulation shows under prediction of the maximum temperature, the UMD simulation tends to over predict the maximum. On the other hand, the minimum temperature shows slight under prediction in the case of UMD simulation while the MCNC simulation shows over prediction. Examination of the bias shows that the UMD excursions are higher in magnitude than the over- or under- prediction of MCNC, although the magnitude of the under predictions are about the same.

Spatial correlation

We also examined the correlation of meteorological parameters between model simulated and measured (TDL and CASTNet) data for each of the monitors. The total number of locations considered in this analysis, are 98 and 14 for the TDL and CASTNet, respectively.

Figures 13, 14, and 15 display spatial distribution of correlation for wind speed, temperature, and mixing ratio, respectively, between TDL based-data and MCNC's MM5 simulation. Similarly, Figures 16, 17, and 18 display the correlation for wind speed, temperature and mixing ratio, respectively for the UMD's MM5 simulation. In the case of temperature (see Figures 14 and 17) the UMD simulation appears to yield higher correlation than the MCNC simulation, while for wind speed (see Figure 13 and 16) both simulations exhibit similar level of correlation. In the case of mixing ratio (See Figures 15 and 18) there appears to be slightly higher level of correlation for the MCNC simulation than UMD.

Figures 19 through 22 display the spatial distribution of correlation for wind speed and temperature between CASTNet and the two MM5 simulations. As noted above the sample of stations is much smaller compared to the TDL data. Interestingly, both simulations exhibit lower level of correlation for temperature (see Figures 20 and 22) and for the wind speed (see Figures 19 and 21) when compared to the TDL data.

Discussion and Summary

Both MM5 simulations utilized observational nudging which was based upon TDL data, but not on the measurements from CASTNet. Thus in a way CASTNet provides for an independent assessment, although the number of stations is quite limited in the present assessment.

The agreement between the MM5 simulations is quite good, even though both simulations were conducted independently with differing vertical grid structure. For example, the layer-1 heights are 38m and 20m for MCNC and UMD simulations, respectively. Also, no adjustments were made to the model estimates for monitor height which in the case of temperature probe is about 2m and wind speed and direction at 10m for TDL and for CASTNet at 9m for temperature and 10m for wind speed and direction.

The lack of a better agreement between the model estimated and measured mixing ratio suggests that there is a need for further examination of the methods used for the estimation of the parameter.

Figure 1

MM5 Modeling Domain used in MCNC Simulation

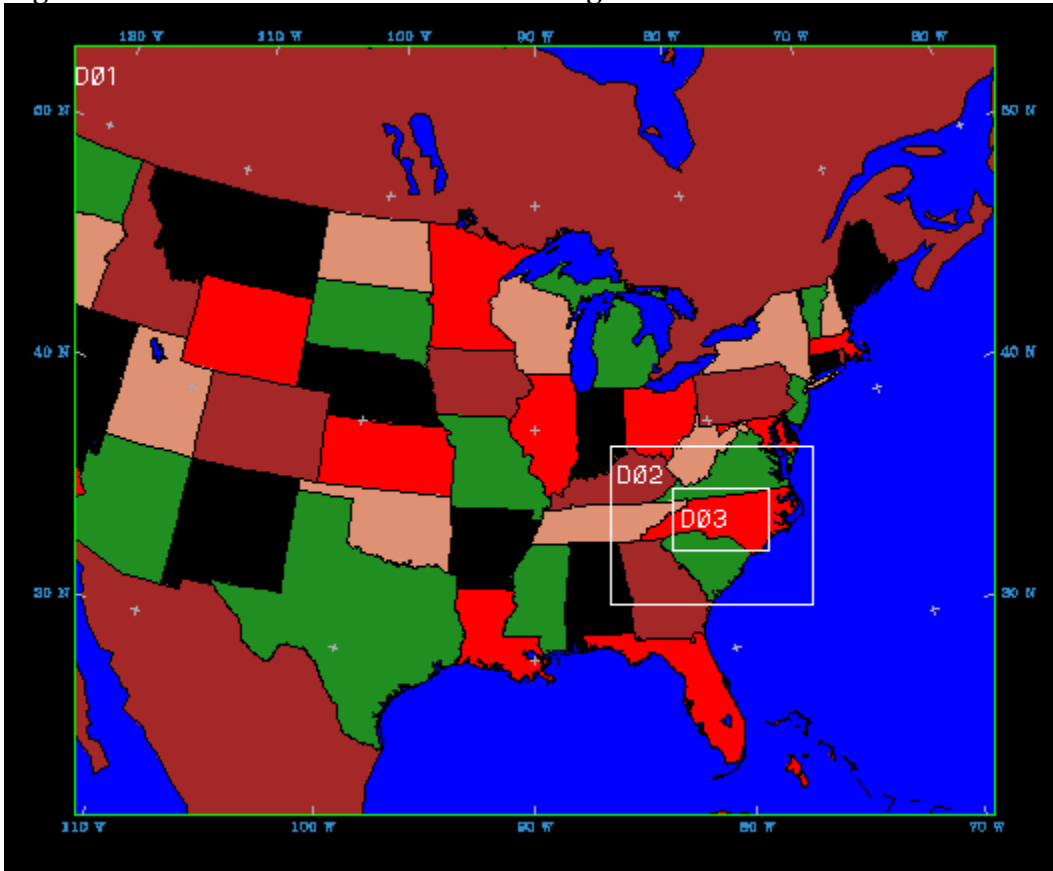


Figure 2

MM5 Modeling Domain used in UMD Simulation

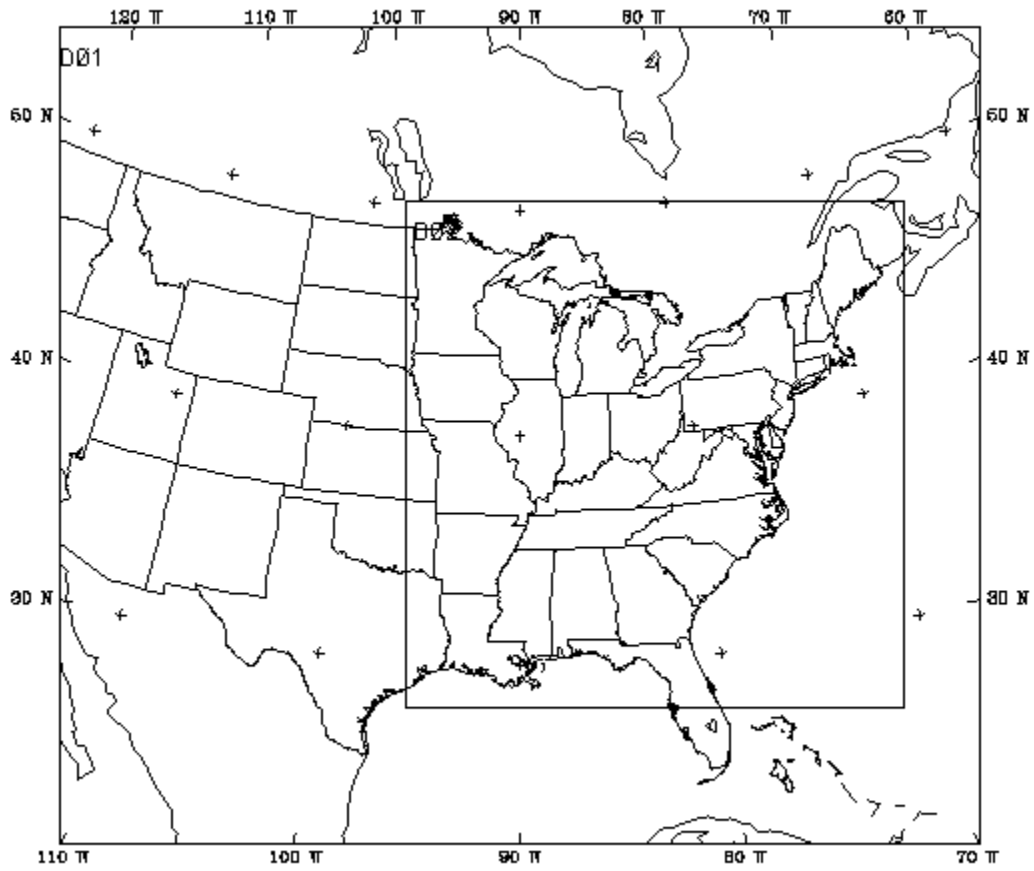


Figure 3

MM5 by MCNC domain2e July 11 to July 15 1997 vs TDL

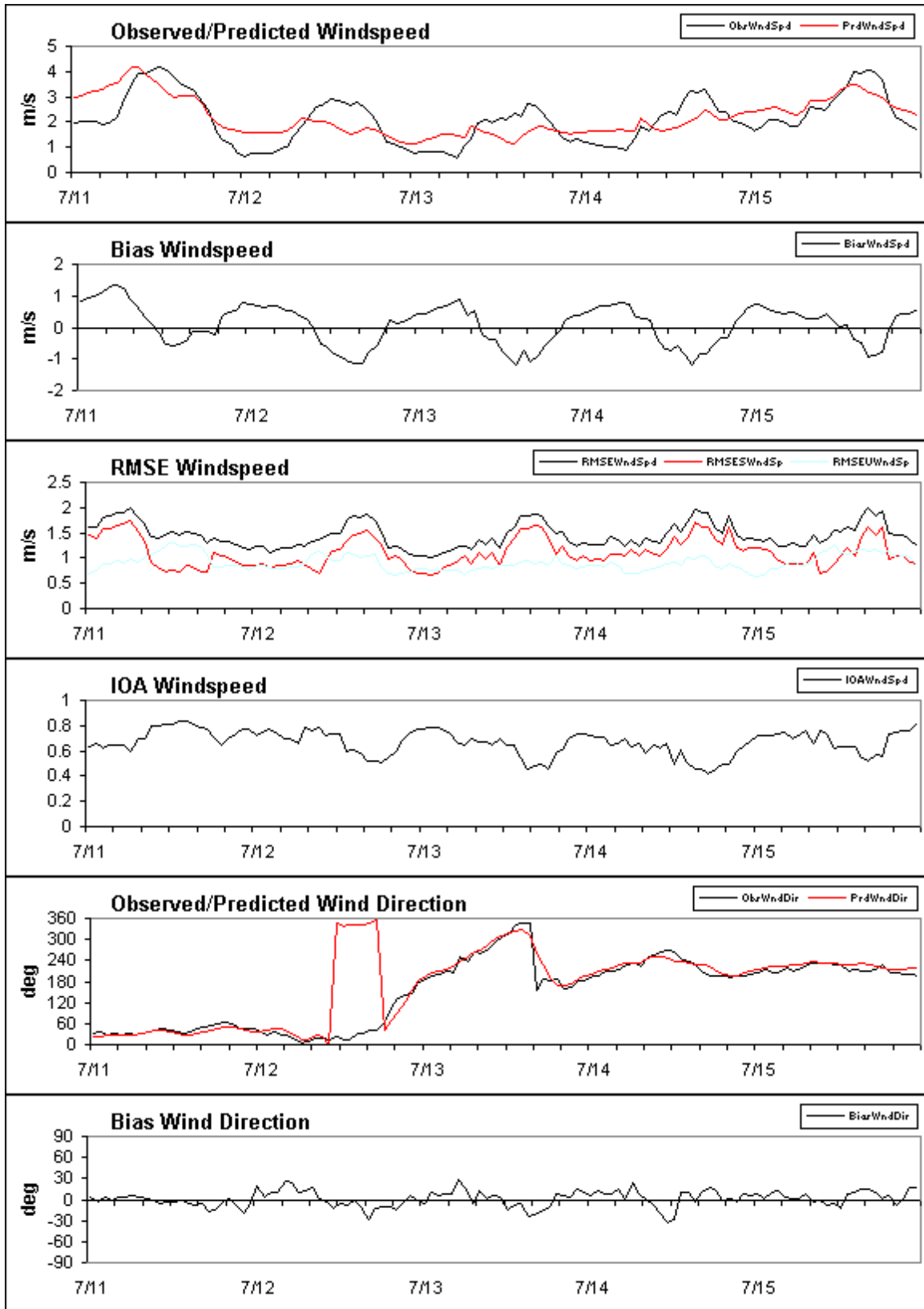


Figure 4

MM5 by UMD domain2e July 11 to July 15 1997 vs TDL

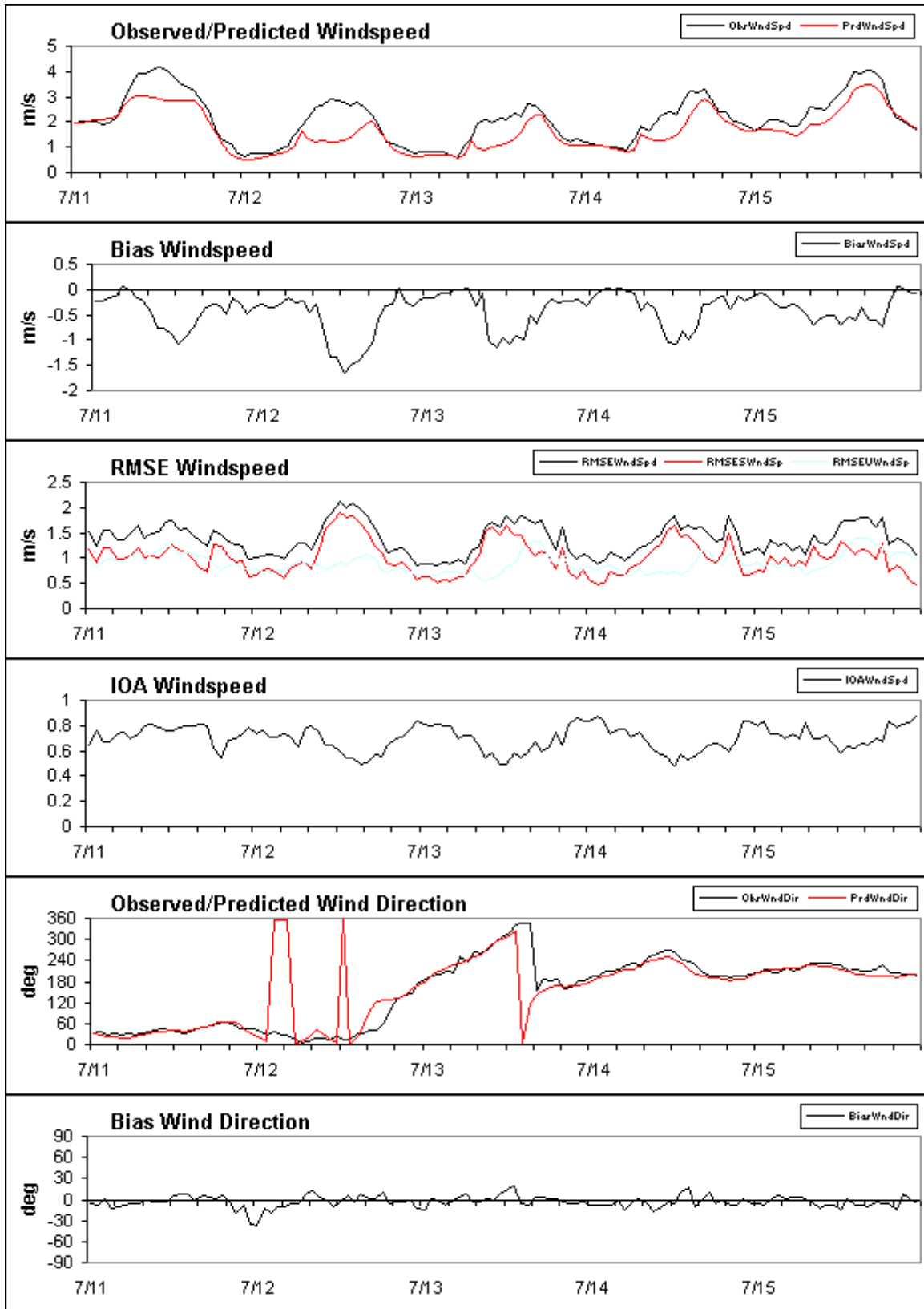


Figure 5 MM5 by MCNC domain2e July 11 to July 15 1997 vs TDL

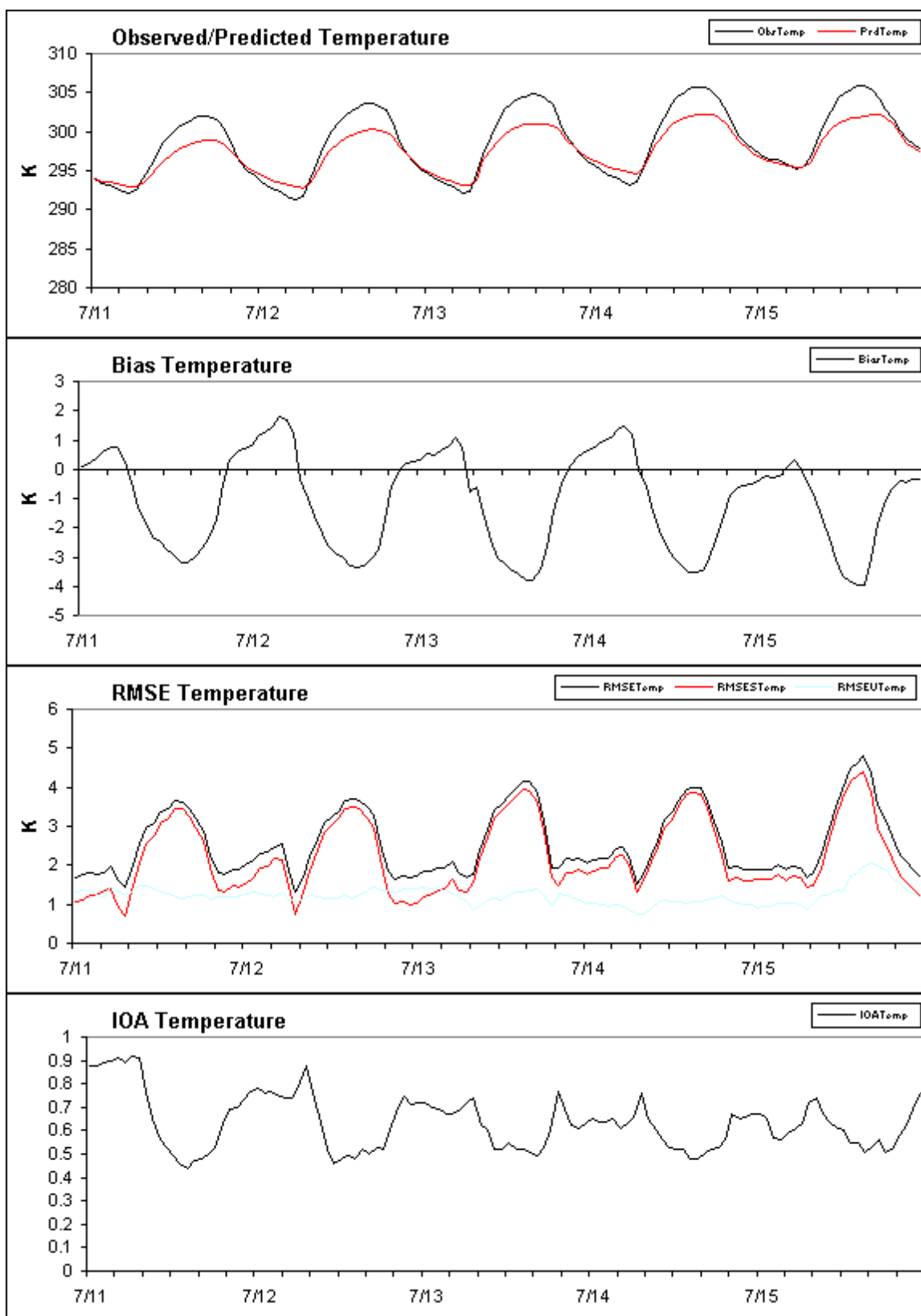


Figure 6 MM5 by UMD domain2e July 11 to July 15 1997 vs TDL

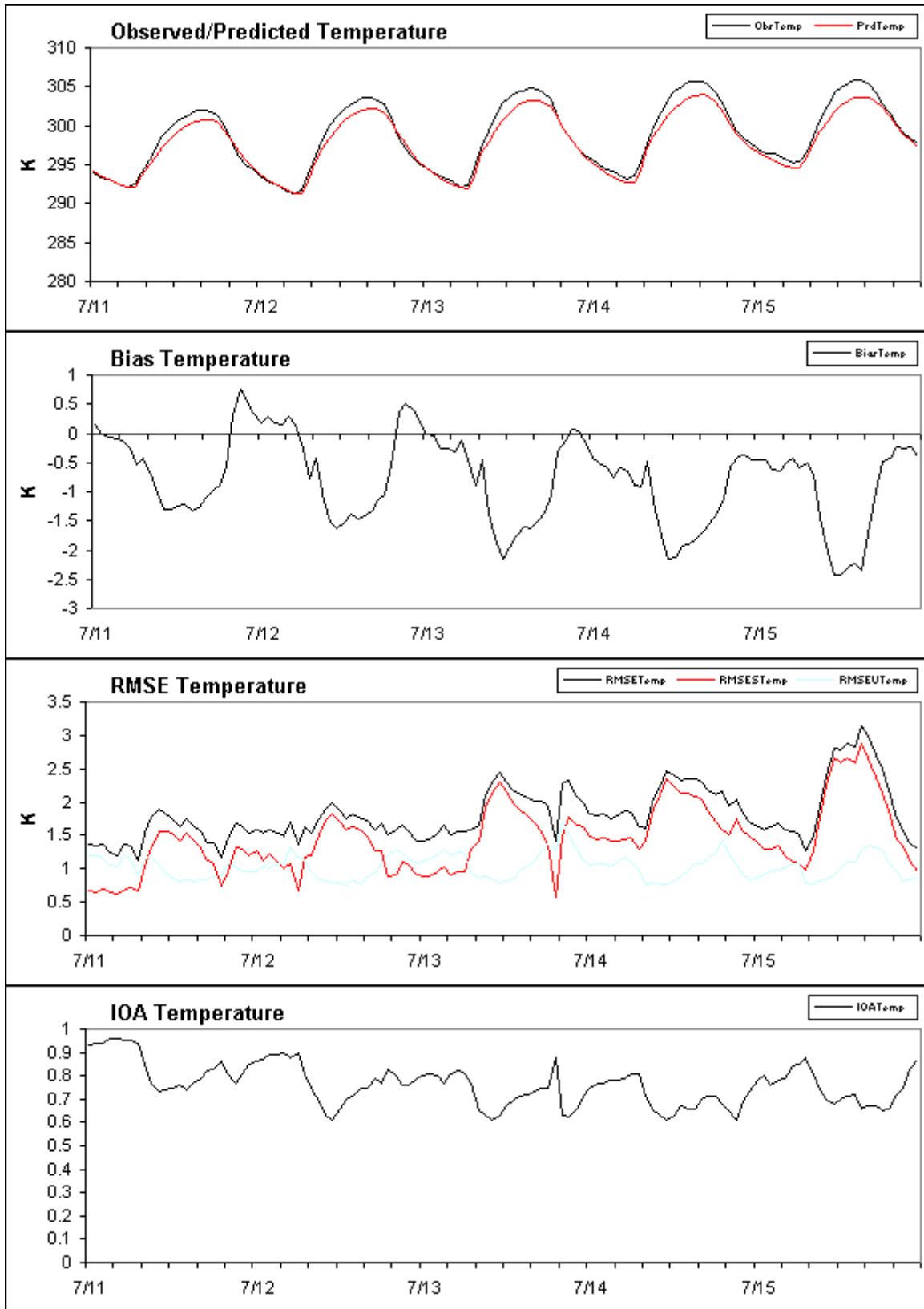


Figure 7

MM5 by MCNC domain2e July 11 to July 15 1997 vs TDL

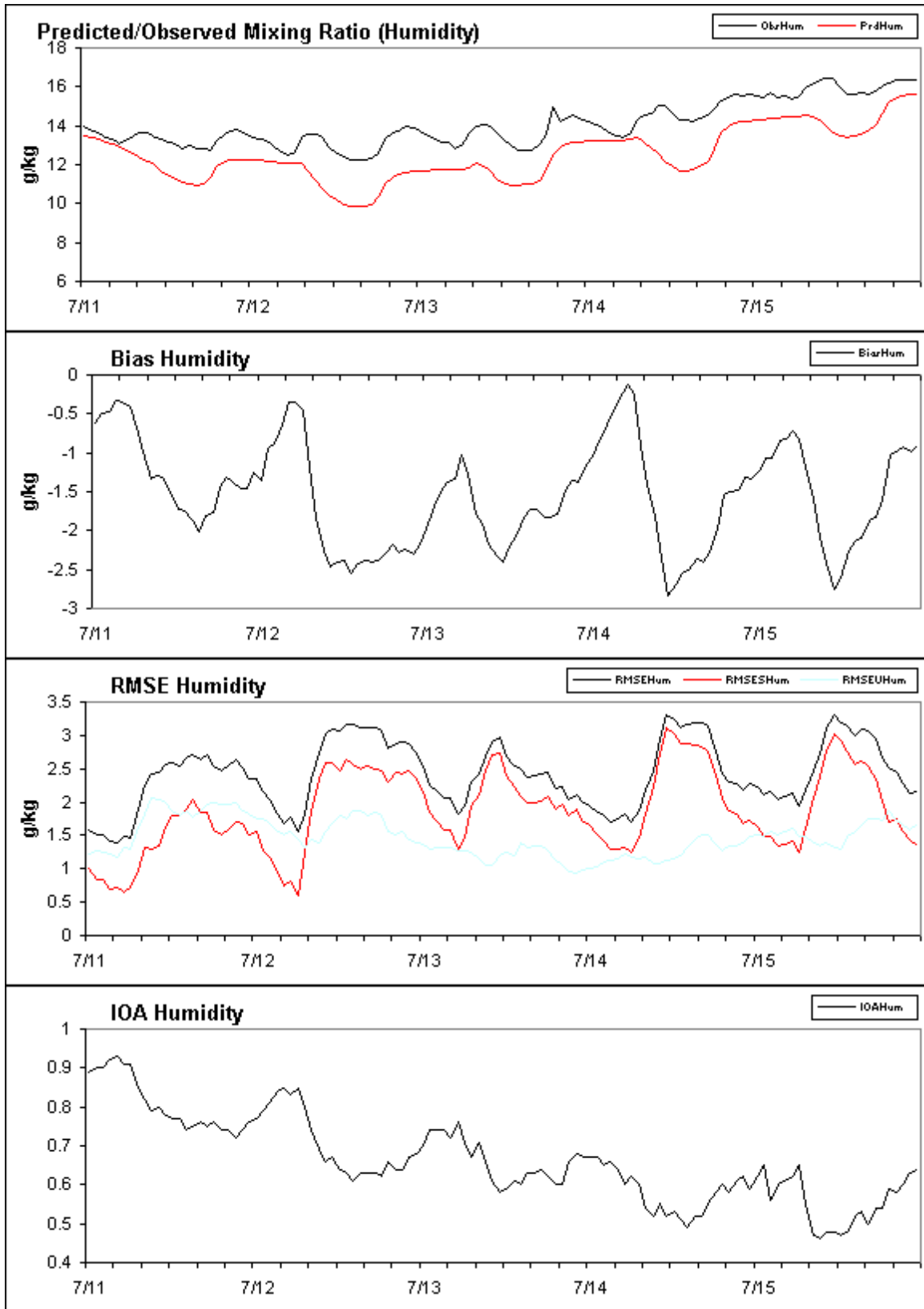


Figure 8 MM5 by UMD domain2e July 11 to July 15 1997 vs TDL

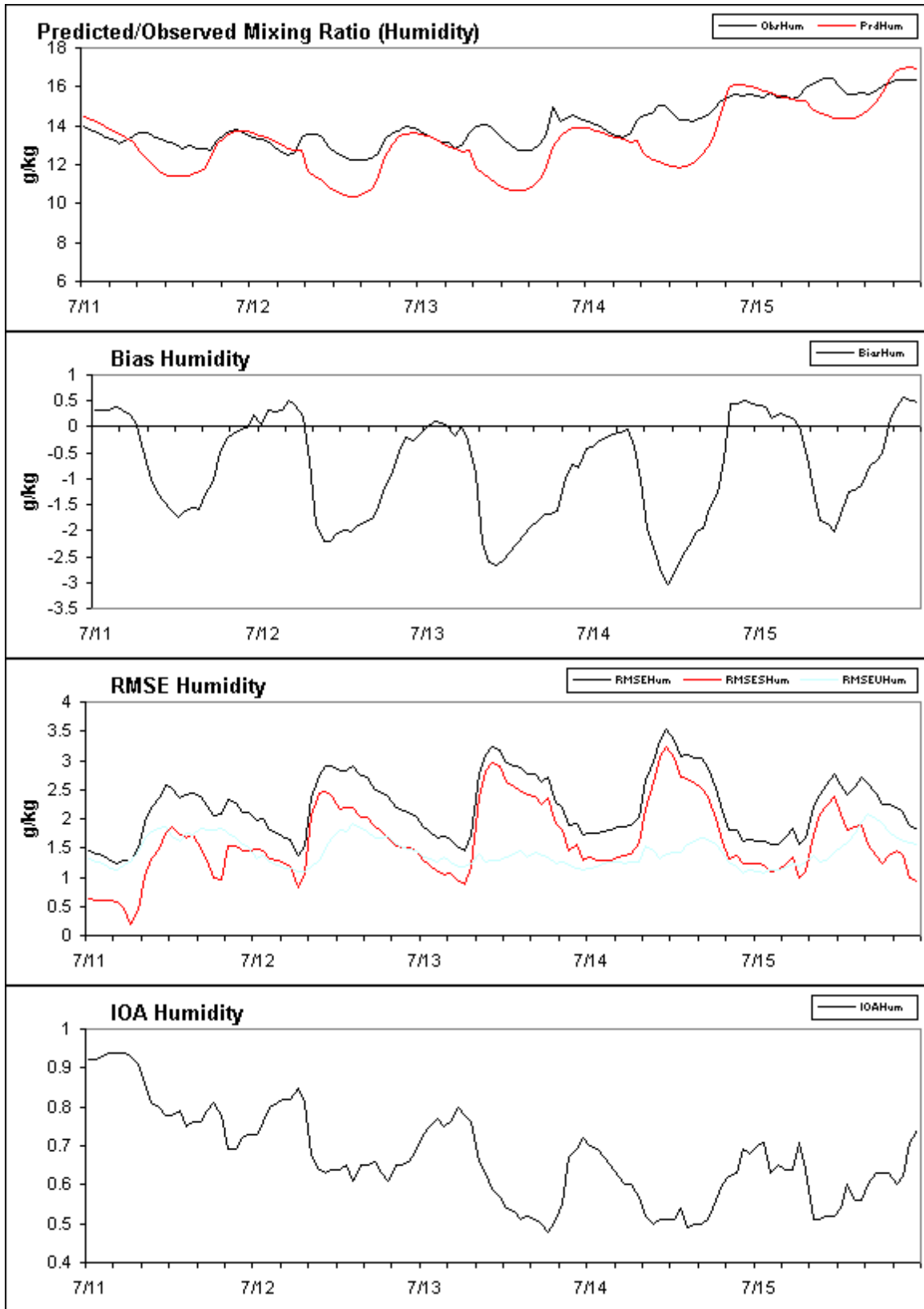


Figure 9 MM5 by MCNC domain2e July 11 to July 15 1997 vs CASTNet

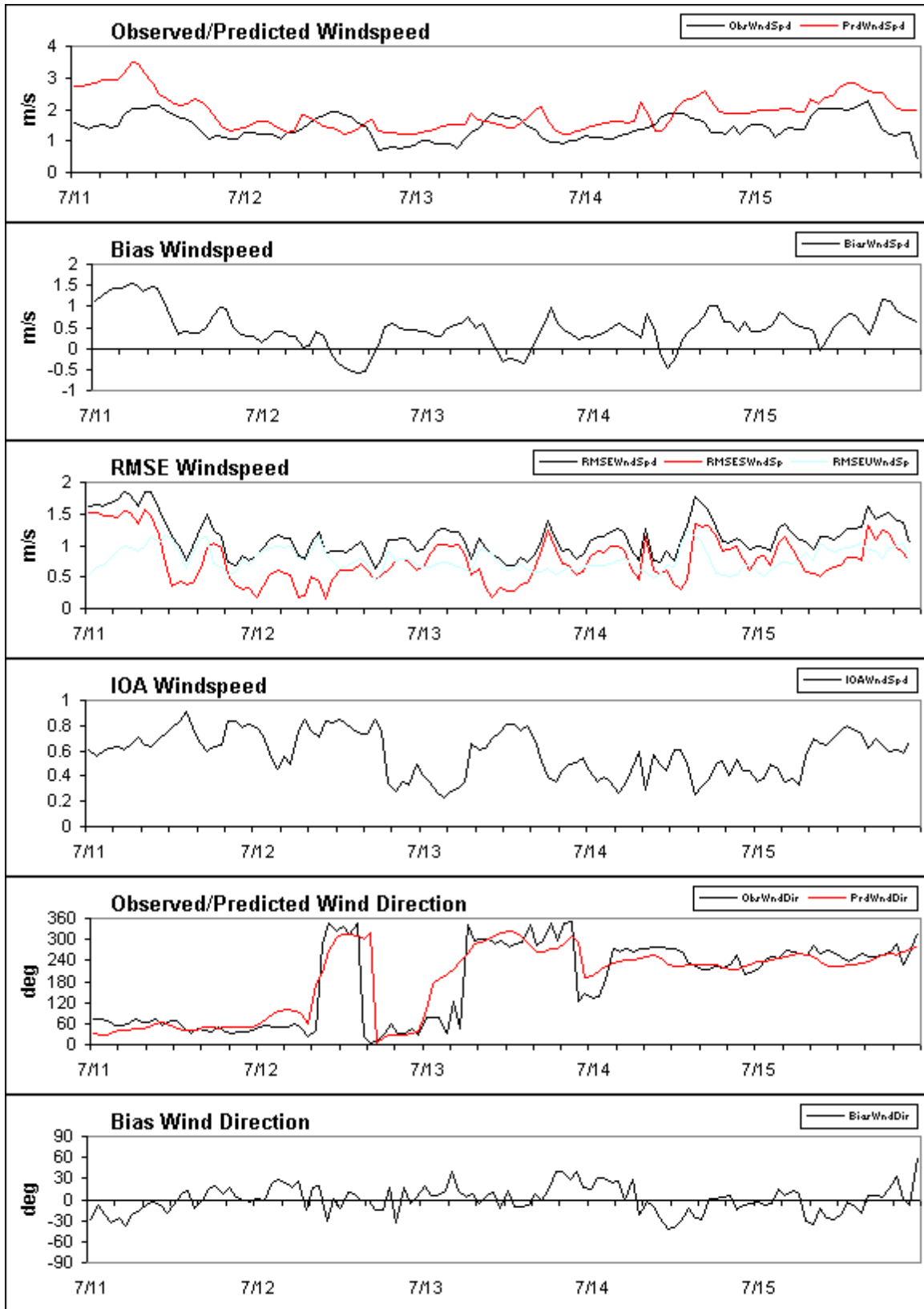


Figure 10 MM5 by UMD domain2e July 11 to July 15 1997 vs CASTNet

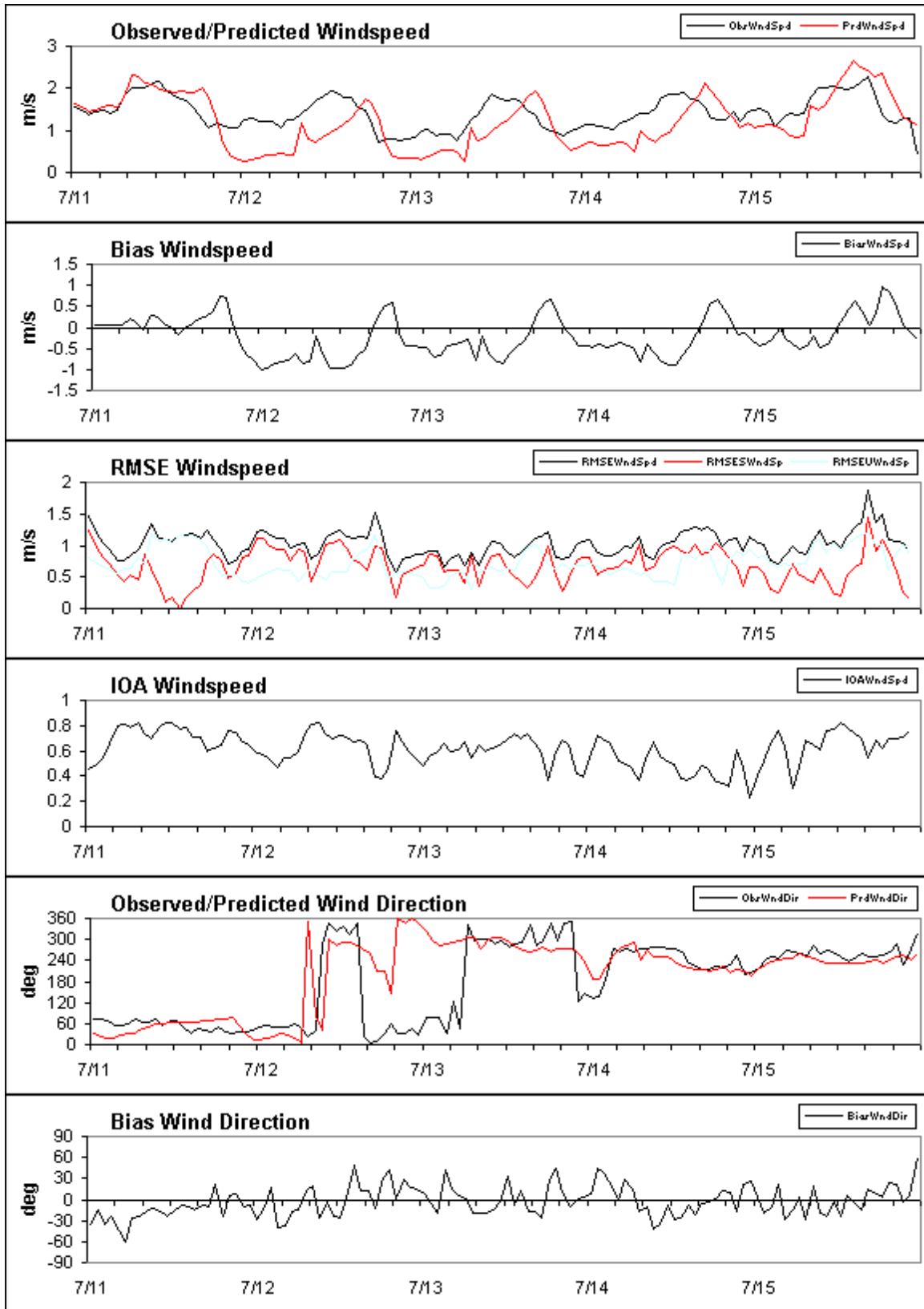


Figure 11 MM5 by MCNC domain2e July 11 to July 15 1997 vs CASTNet

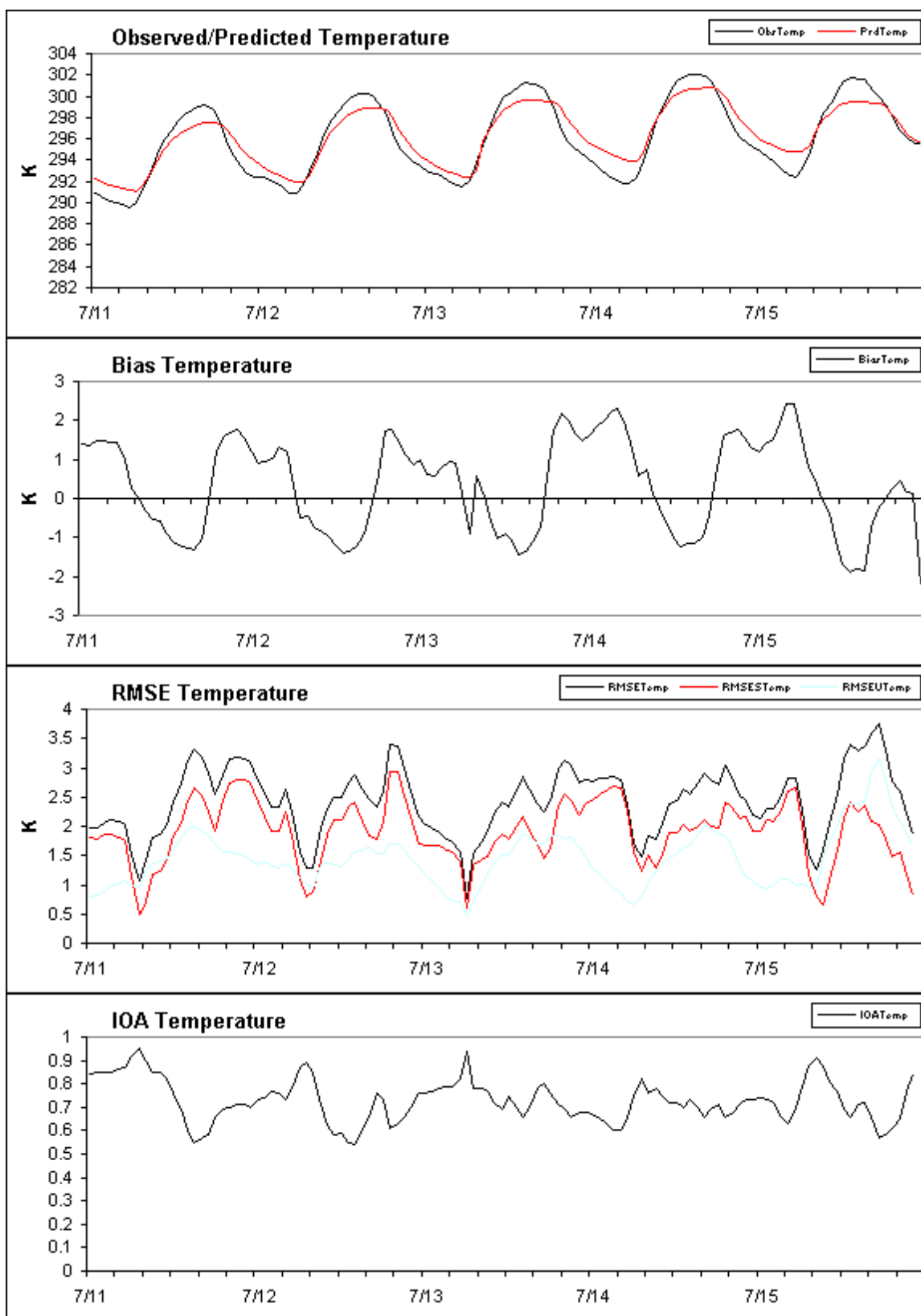


Figure 12 MM5 by UMD domain2e July 11 to July 15 1997 vs CASTNet

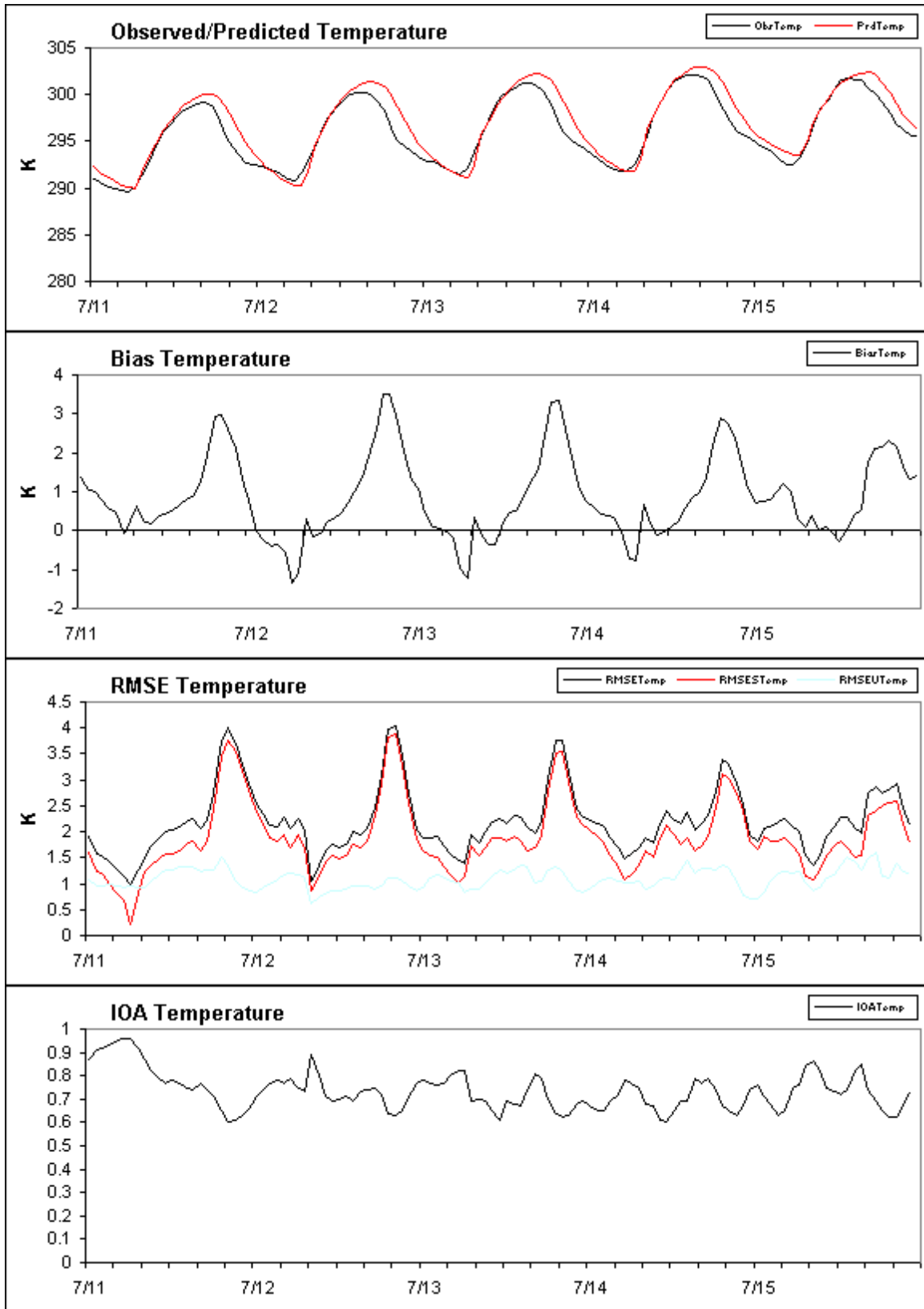


Figure 13 Spatial distribution of correlation for wind speed between TDL and MCNC's MM5 prediction

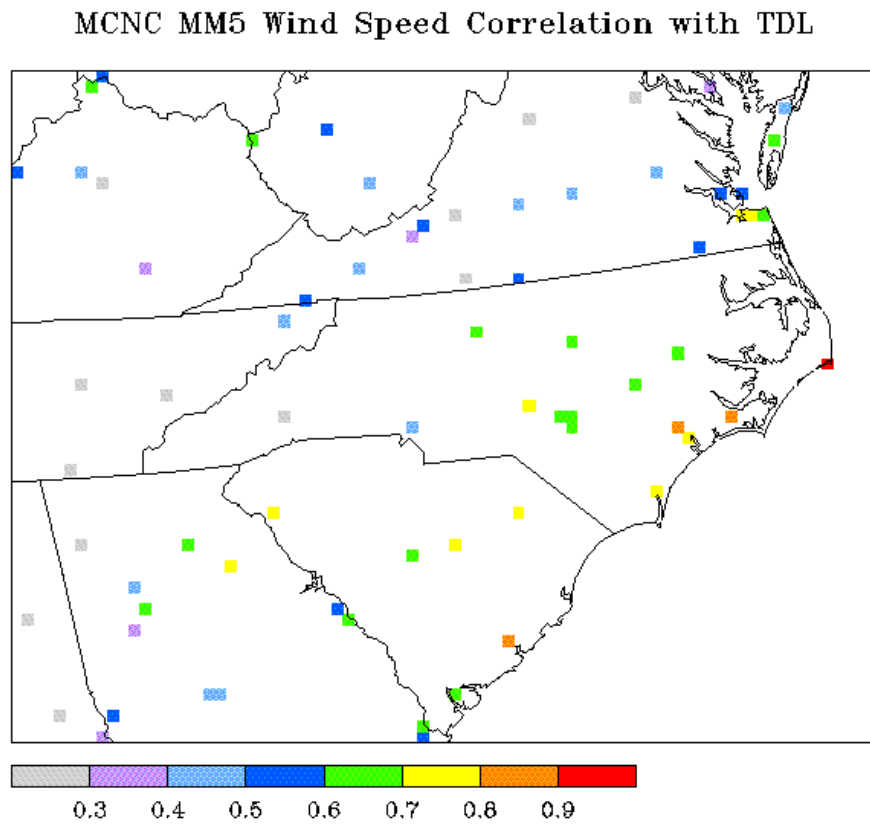


Figure 14 Spatial distribution of correlation for temperature between TDL and MCNC's MM5 prediction

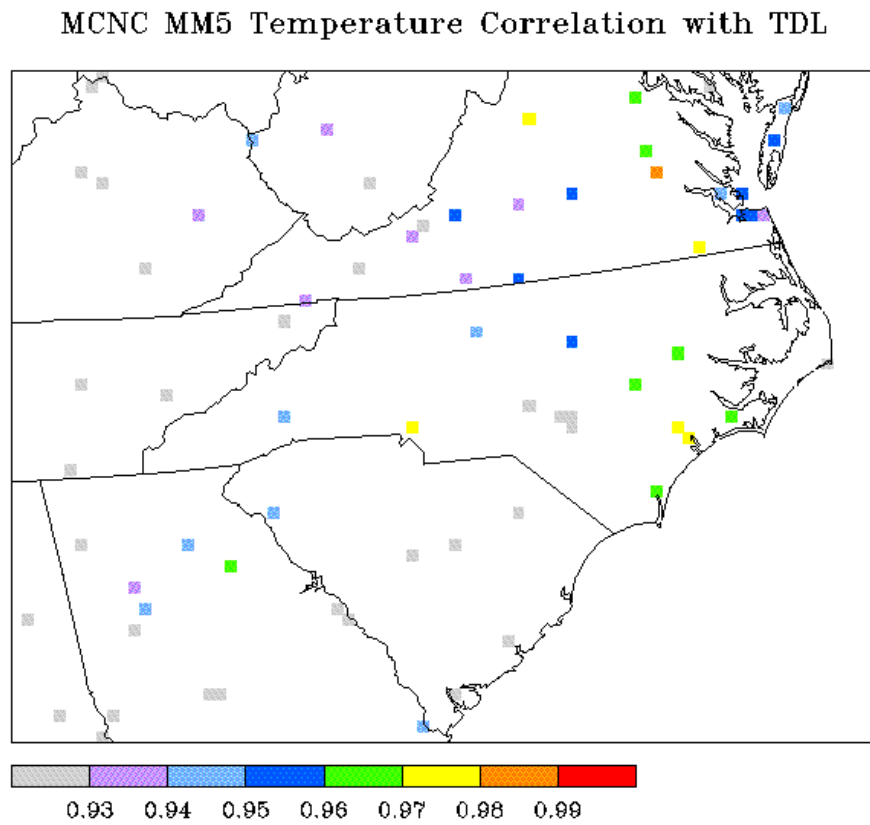


Figure 15 Spatial distribution of correlation for mixing ratio (humidity) between TDL and MCNC's MM5 prediction

MCNC MM5 Mixing Ratio Correlation with TDL

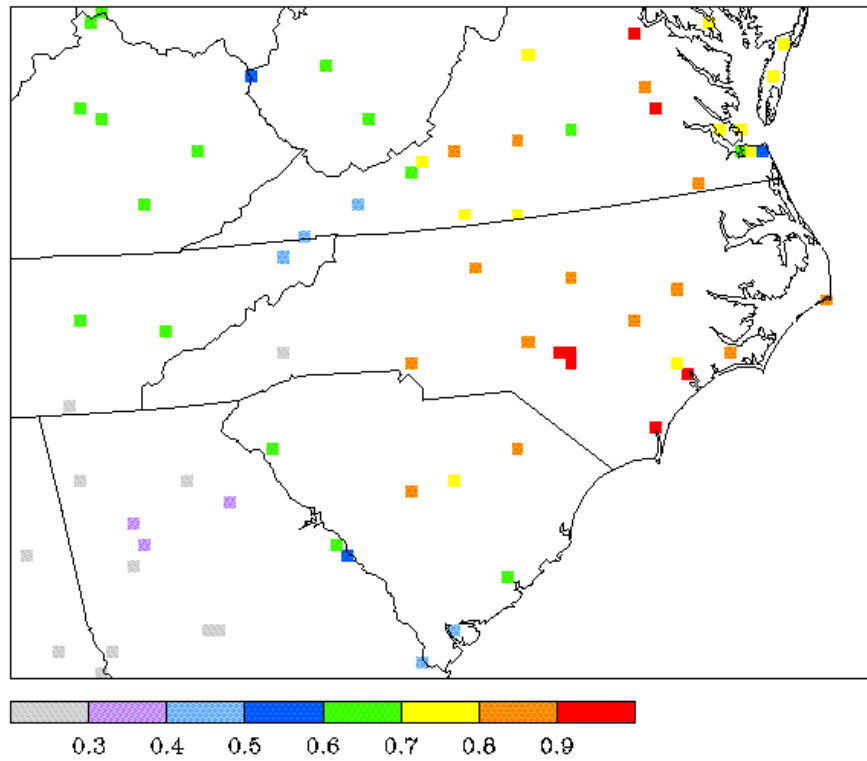


Figure 16 Spatial distribution of correlation for wind speed between TDL and UMD's MM5 prediction

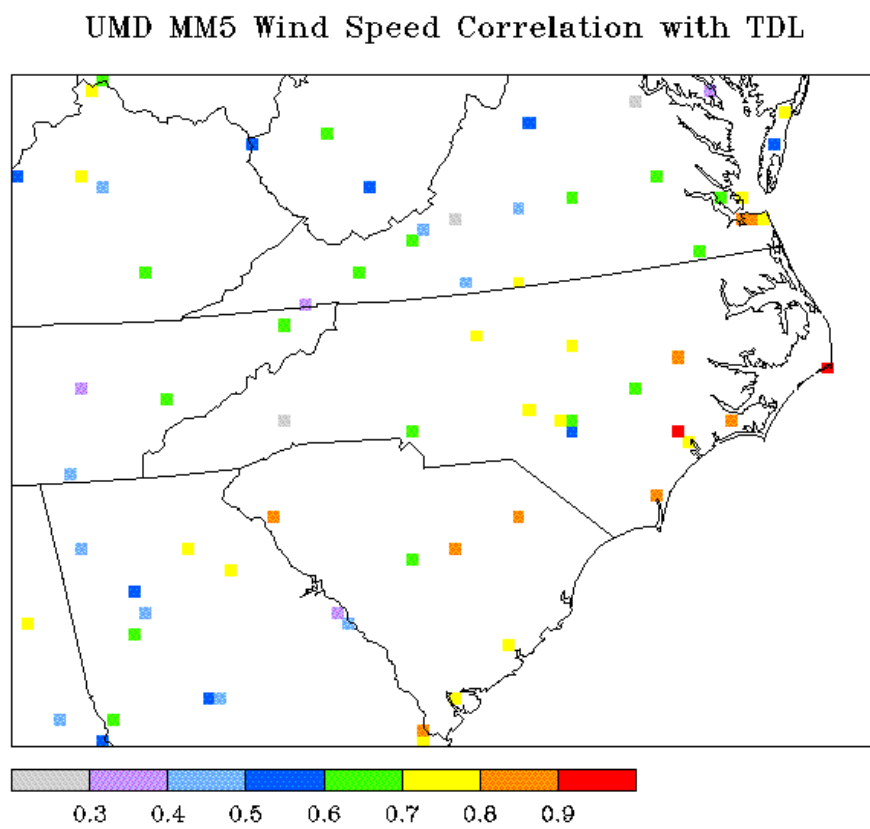


Figure 17 Spatial distribution of correlation for temperature between TDL and UMD's MM5 prediction

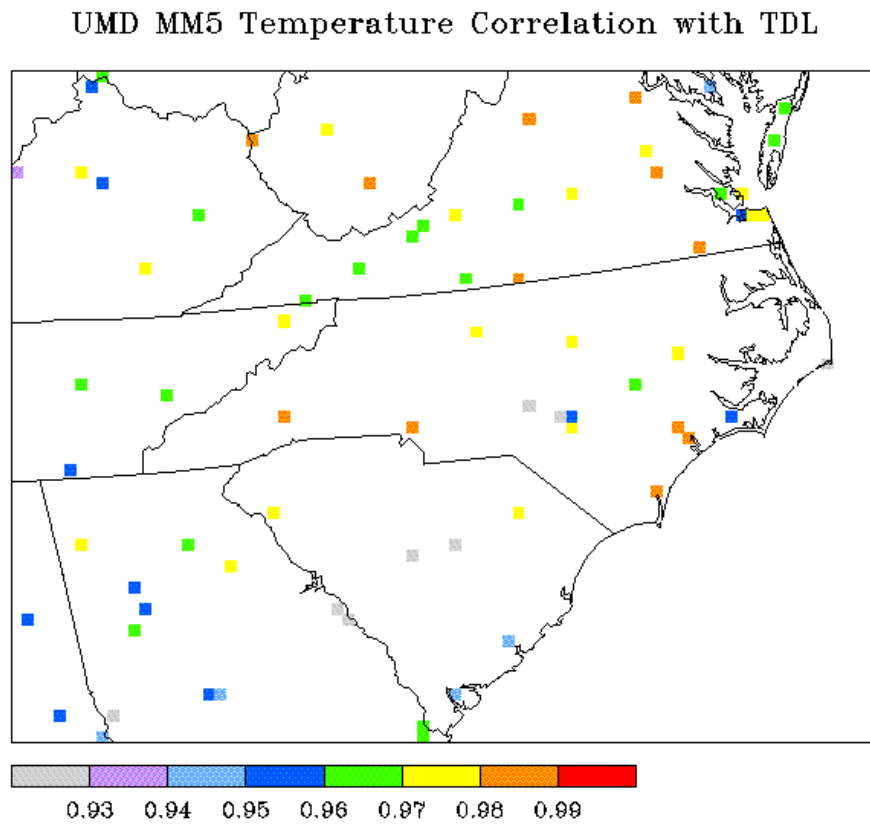


Figure 18 Spatial distribution of correlation for mixing ratio (humidity) between TDL and UMD's MM5 prediction

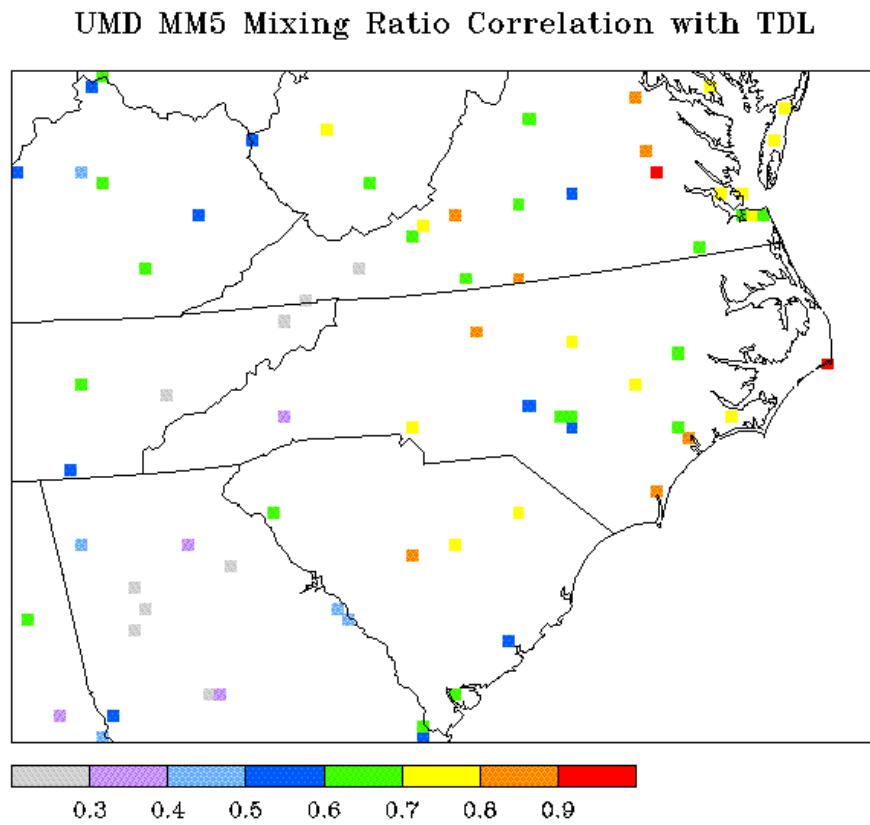


Figure 19 Spatial distribution of correlation for wind speed between CASTNet and MCNC's MM5 prediction

MCNC MM5 Wind Speed Correlation with CASTNet

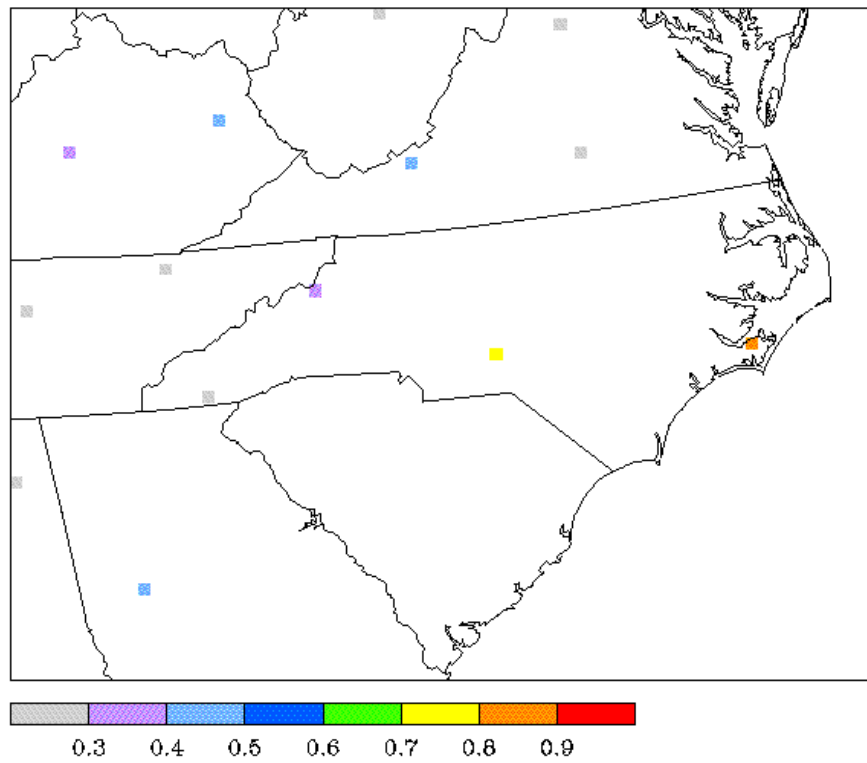


Figure 20 Spatial distribution of correlation for temperature between CASTNet and MCNC's MM5 prediction

MCNC MM5 Temperature Correlation with CASTNet

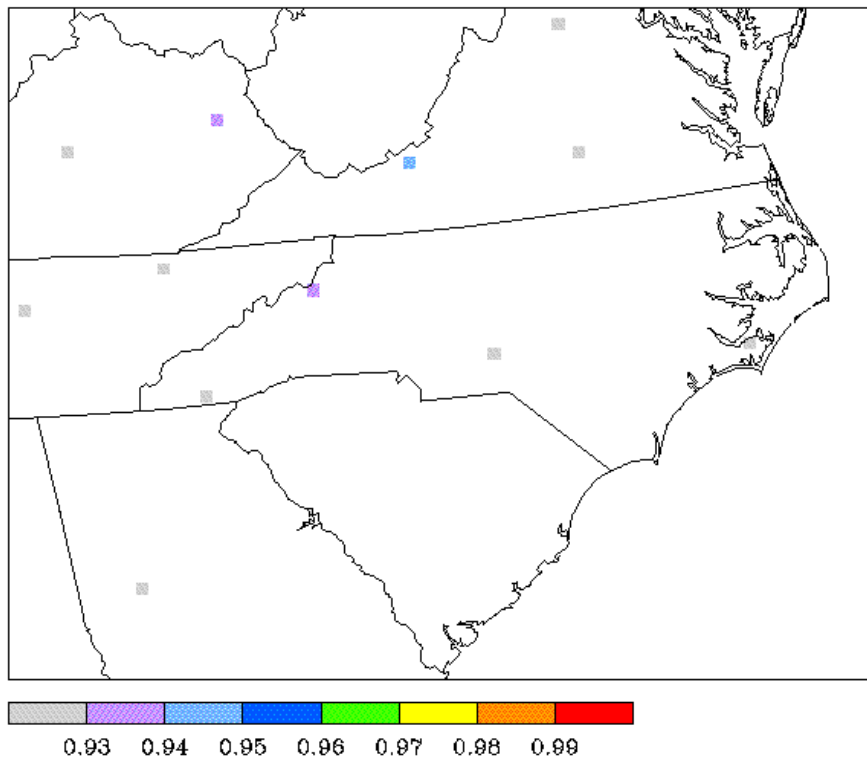


Figure 21 Spatial distribution of correlation for wind speed between CASTNet and UMD's MM5 prediction

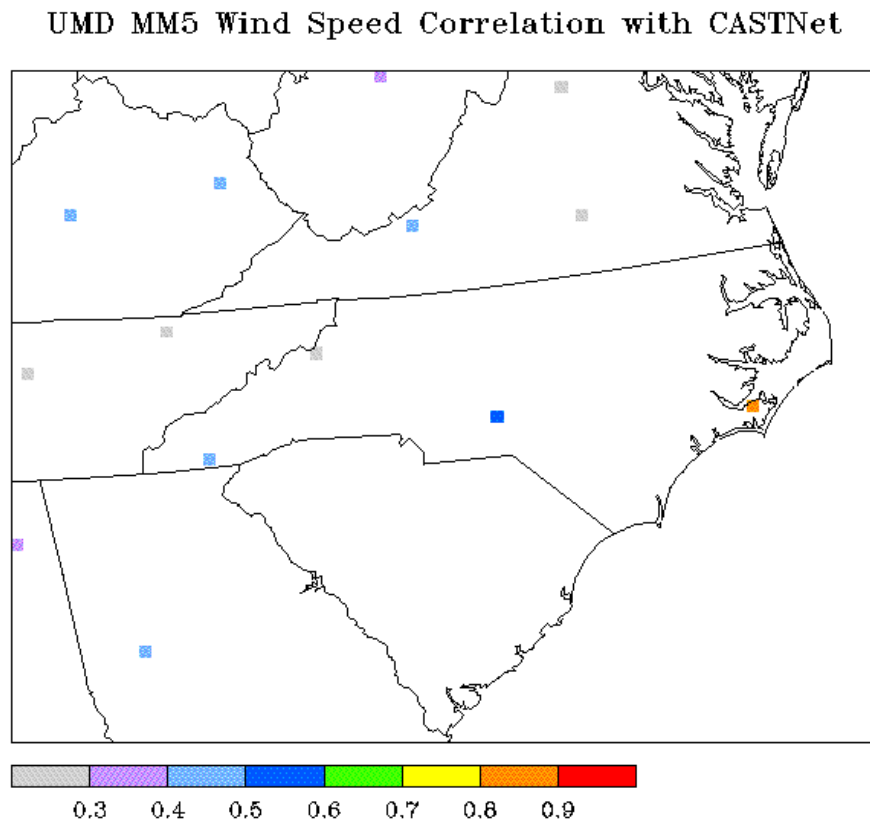


Figure 22 Spatial distribution of correlation for temperature between CASTNet and UMD's MM5 prediction

UMD MM5 Temperature Correlation with CASTNet

